

THE STRETCH FACTOR OF THE DELAUNAY TRIANGULATION IS LESS THAN 1.998*

GE XIA[†]

Abstract. Let S be a finite set of points in the Euclidean plane. Let D be a Delaunay triangulation of S . The *stretch factor* (also known as *dilation* or *spanning ratio*) of D is the maximum ratio, among all points p and q in S , of the shortest path distance from p to q in D over the Euclidean distance $\|pq\|$. Proving a tight bound on the stretch factor of the Delaunay triangulation has been a long-standing open problem in computational geometry. In this paper we prove that the stretch factor of the Delaunay triangulation is less than $\rho = 1.998$, significantly improving the current best upper bound of 2.42 by Keil and Gutwin [“The Delaunay triangulation closely approximates the complete Euclidean graph,” in Proceedings of the 1st Workshop on Algorithms and Data Structures (WADS), 1989, pp. 47–56]. Our bound of 1.998 also improves the upper bound of the best stretch factor that can be achieved by a plane spanner of a Euclidean graph (the current best upper bound is 2). Our result has a direct impact on the problem of constructing spanners of Euclidean graphs, which has applications in the area of wireless computing.

Key words. Delaunay triangulation, stretch factor, dilation, spanning ratio, spanners

AMS subject classifications. 65D18, 68U05, 52C99

DOI. 10.1137/110832458

1. Introduction. Let S be a finite set of points in the Euclidean plane. A *Delaunay triangulation* of S is a triangulation in which the circumscribed circle of every triangle contains no point of S in its interior. An alternative equivalent definition is the following: An edge xy is in the Delaunay triangulation of S if and only if there is a circle through points x and y whose interior is devoid of points of S . A Delaunay triangulation of S is the dual graph of the Voronoi diagram of S .

Let D be a Delaunay triangulation of S . The *stretch factor* (also known as *dilation* or *spanning ratio*) of D is the maximum ratio, among all points p and q in S , of the shortest path distance from p to q in D over the Euclidean distance $\|pq\|$.

Proving a tight bound on the stretch factor of the Delaunay triangulation has been a long-standing open problem in computational geometry. Chew [5] showed a lower bound of $\pi/2$ on the stretch factor of the Delaunay triangulation. This lower bound of $\pi/2$ was widely believed to be tight until recently (2009) when Bose et al. [2] proved that the lower bound is at least $1.5846 > \pi/2$, which was further improved to 1.5932 by Xia and Zhang [17]. Dobkin, Friedman, and Supowit [7, 8] in 1987 showed that the Delaunay triangulation has stretch factor at most $(1 + \sqrt{5})\pi/2 \approx 5.08$. This upper bound was improved by Keil and Gutwin [12, 13] in 1989 to $2\pi/(3 \cos(\pi/6)) \approx 2.42$. Despite considerable efforts since then, 2.42 currently stands as the best upper bound on the stretch factor of the Delaunay triangulation. For the special case when the point set S is in convex position, Cui, Kanj, and Xia [6] recently proved that the Delaunay triangulation of S has stretch factor at most 2.33.

In this paper we prove that the stretch factor of the Delaunay triangulation of a point set in the plane is less than $\rho = 1.998$, significantly improving the current best

*Received by the editors April 29, 2011; accepted for publication (in revised form) May 7, 2013; published electronically July 30, 2013. The preliminary version of the paper appears in *Proceedings of the 27th Annual Symposium on Computational Geometry* (SoCG 2011). This work was supported in part by a Lafayette College research grant.

<http://www.siam.org/journals/sicomp/42-4/83245.html>

[†]Department of Computer Science, Lafayette College, Easton, PA 18042 (xiag@lafayette.edu).

upper bound of 2.42 from 1989 [12, 13]. Our bound of 1.998 is also better than the upper bound of 2.33 for the special case when the point set is in convex position [6].

Our approach in proving the upper bound on the stretch factor of the Delaunay triangulation is different from the previous approaches [7, 8, 12, 13, 6]. Our approach focuses on the geometry of a “chain” of disks in the plane (the formal definition of the chain is given in section 2). The “stretch factor” of a chain can be defined in analogy to that of the Delaunay triangulation. We prove that the upper bound on the stretch factor of a chain is less than 1.998.

THEOREM 1. *The stretch factor of a chain of disks \mathcal{O} in the plane is less than $\rho = 1.998$.*

As a special case of Theorem 1, we derive the same upper bound on the stretch factor of the Delaunay triangulation.

COROLLARY 1. *The stretch factor of a Delaunay triangulation D of a set of points S in the plane is less than $\rho = 1.998$.*

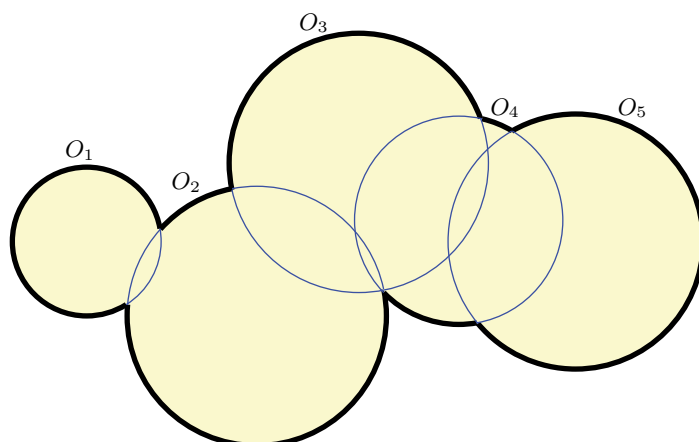
Our result has a direct impact on the problem of constructing *spanners* of Euclidean graphs [4], which has applications in the area of wireless computing (for more details, see [15]). Many spanner constructions in the literature rely on extracting subgraphs of the Delaunay triangulation (see, for example, [3, 9, 10, 14]) and their spanning ratio is expressed as a function of the stretch factor of the Delaunay triangulation. Hence the new upper bound of 1.998 on the stretch factor of the Delaunay triangulation automatically improves the upper bounds on the spanning ratio of all such spanners.

Another important consequence of our result is that it improves the upper bound of the best stretch factor achieved by plane spanners of the complete two-dimensional Euclidean graph. Previously, the plane spanner with the best known upper bound on the stretch factor is the triangular distance Delaunay triangulation by Chew [5], whose stretch factor is 2. Our result shows that the Delaunay triangulation has a smaller upper bound of 1.998 on the stretch factor.

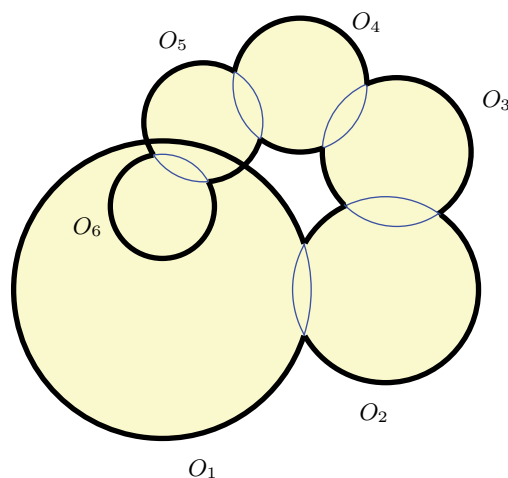
We believe that future research based on our approach will yield further improvements in both the upper and lower bounds, and may eventually lead to the tight bound of the stretch factor of the Delaunay triangulation. At the end of this paper, we will discuss possible ways to improve our approach for a better upper bound. Following our approach, Xia and Zhang [17] showed an improved lower bound of 1.5932 for the stretch factor of the Delaunay triangulation by giving a sequence of chains with increasing stretch factors. It was conjectured in [17] that the tight bound occurs at the limit of the sequence.

The paper is organized as follows. The necessary definitions are given in section 2. The main theorem of the paper is presented in section 3. There we also discuss the proof strategy and provide an outline of the proof for the main theorem. Most of the technical details are captured by two lemmas, whose proofs appear in sections 4 and 5. We discuss the possible improvements of our approach in section 6. Section 7 (the appendix) contains the proofs of some claims made in the paper.

2. Preliminaries. We label the points in the plane by lowercase letters, such as p, q, u, v , etc. For any two points p, q in the plane, denote by pq the line in the plane passing through p and q , by \overline{pq} the line segment connecting p and q , and by \vec{pq} the ray from p to q . The Euclidean distance between p and q is denoted by $\|pq\|$. The length of a path P in the plane is denoted by $|P|$. Any angle denoted by $\angle poq$ is measured from \vec{op} to \vec{oq} in the *counterclockwise* direction. Unless otherwise specified, all angles in this paper are defined in the range $(-\pi, \pi]$.



(a) Example 1.



(b) Example 2.

FIG. 1. Examples of chains. The connecting arcs are thin. A chain may self-intersect, as in Example 2. Although O_1 and O_5 intersect in Example 2, there are no connecting arcs between them because they are not consecutive in the sequence.

DEFINITION 1. We say that a finite sequence of distinct disks¹ $\mathcal{O} = (O_1, O_2, \dots, O_n)$ in the plane is a chain if it has the following two properties: (1) Every two consecutive disks O_i, O_{i+1} intersect,² $1 \leq i \leq n - 1$, but neither disk contains the other. Denote by $C_i^{(i-1)}$ and $C_i^{(i+1)}$ the arcs on the boundary of O_i that is in O_{i-1} and O_{i+1} , respectively. We refer to $C_i^{(i-1)}$ and $C_i^{(i+1)}$ as the “connecting arcs” of O_i . (2) The connecting arcs $C_i^{(i-1)}$ and $C_i^{(i+1)}$ of O_i do not overlap for $2 \leq i \leq n - 1$; however, $C_i^{(i-1)}$ and $C_i^{(i+1)}$ can share an endpoint. See Figure 1 for an illustration. For any $1 \leq i \leq j \leq n$, denote by $\mathcal{O}_{i,j}$ a subchain of \mathcal{O} : $\mathcal{O}_{i,j} = (O_i, \dots, O_j)$.

¹In this paper, a disk is considered to be a closed subset of the plane.

²This includes the case where O_i, O_{i+1} are tangent.

DEFINITION 2. Given a chain $\mathcal{O} = (O_1, O_2, \dots, O_n)$. Let u be a point on the boundary of O_1 that is not in the interior of O_2 . Let v be a point on the boundary of O_n that is not in the interior of O_{n-1} . We call u, v a pair of terminal points (or simply terminals) of the chain \mathcal{O} . Let o_1, \dots, o_n be the centers of O_1, \dots, O_n , respectively. We call the polyline $uo_1 \dots o_nv$ the centered polyline between u and v . For $1 \leq i \leq n - 1$, let a_i and b_i be the intersections of the boundaries of O_i and O_{i+1} (in the special case where O_i, O_{i+1} are tangent, $a_i = b_i$). Without loss of generality, assume all a_i 's are on one side of the centered polyline $uo_1 \dots o_nv$ and all b_i 's are on the other side³ (if $a_i = b_i$ then both of them are on the centered polyline). For notational convenience, define $a_0 = b_0 = u$ and $a_n = b_n = v$. Every disk O_i has two arcs on its boundary between the line segments $\overline{a_{i-1}b_{i-1}}$ and $\overline{a_i b_i}$, denoted by A_i and B_i . Without loss of generality, assume that a_{i-1}, a_i are the ends of A_i and b_{i-1}, b_i are the ends of B_i for $1 \leq i \leq n$. This means that $A_1 \dots A_n$ is a path from u to v on one side of the chain and $B_1 \dots B_n$ is a path from u to v on the other side of the chain. An arc A_i or B_i may degenerate to a point, in which case $a_{i-1} = a_i$ or $b_{i-1} = b_i$, respectively. Refer to Figure 2 for an illustration.

DEFINITION 3. Let $D_{\mathcal{O}}(u, v) = up_1 \dots p_{n-1}v$ be the shortest polyline from u to v that consists of line segments $\overline{up_1}, \overline{p_1p_2}, \dots, \overline{p_{n-1}v}$, where $p_i \in \overline{a_i b_i}$ for $1 \leq i \leq n - 1$. In other words, the polyline $D_{\mathcal{O}}(u, v)$ is the shortest polyline (which can be visualized as a rubber band) from u to v that intersects line segments $\overline{a_1 b_1}, \dots, \overline{a_{n-1} b_{n-1}}$ in that order. See Figure 2 for an illustration. The length of $D_{\mathcal{O}}(u, v)$, denoted by $|D_{\mathcal{O}}(u, v)|$, is the sum of the lengths of the line segments in $D_{\mathcal{O}}(u, v)$. If the polyline $D_{\mathcal{O}}(u, v)$ contains a point p_j which is a_j or b_j for some $1 \leq j \leq n - 1$, we say that u, v are obstructed. If u, v are unobstructed, then $D_{\mathcal{O}}(u, v)$ is the straight line segment \overline{uv} . Note that the converse of this statement is not true, because even when $D_{\mathcal{O}}(u, v)$ is the straight line segment \overline{uv} , $D_{\mathcal{O}}(u, v)$ may still contain a point $p_j \in \{a_j, b_j\}$. See Figure 2 for an illustrations of obstructed and unobstructed cases.⁴

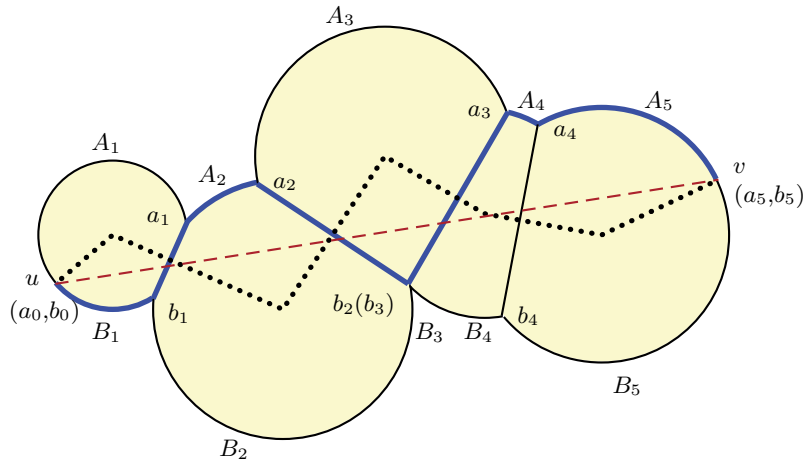
We have the following simple proposition.

PROPOSITION 1. If $D_{\mathcal{O}}(u, v)$ is the straight line segment \overline{uv} , then \overrightarrow{uv} stabs O_1, \dots, O_n in order. That is, for any $1 \leq i < j \leq n$, \overrightarrow{uv} enters O_i no later than entering O_j and exits O_i no later than exiting O_j .

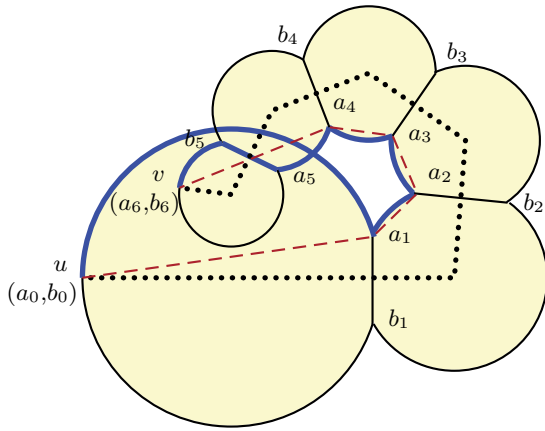
Proof. For $2 \leq i \leq n - 1$, the two connecting arcs on O_i do not overlap. Hence $\overline{a_{i-1}b_{i-1}}$ and $\overline{a_{i+1}b_{i+1}}$ must appear on the different sides of the line $a_i b_i$. Refer to Figure 3. Without loss of generality, assume that $a_i b_i$ is a vertical line which divides the plane into two half-planes so that $\overline{a_{i-1}b_{i-1}}$ appears in the left half-plane and $\overline{a_{i+1}b_{i+1}}$ appears in the right half-plane. If $D_{\mathcal{O}}(u, v)$ is the straight line segment \overline{uv} , then $u, p_1, p_2, \dots, p_{n-1}, v$ are colinear and they appear in that order in the ray \overrightarrow{uv} . This means that \overrightarrow{uv} crosses $\overline{a_i b_i}$ from left to right. Thus \overrightarrow{uv} enters O_{i-1} and O_i in the left half-plane. The line $a_i b_i$ divides O_{i-1} and O_i each into the left portion and the right portion (w.r.t. $a_i b_i$). The left portion of O_i is contained in the left portion of O_{i-1} , and hence \overrightarrow{uv} must enter O_{i-1} no later than entering O_i . Likewise, \overrightarrow{uv} exits O_{i-1} and O_i in the right half-plane. Since the right portion of O_{i-1} is contained in the right portion of O_i , \overrightarrow{uv} must exit O_{i-1} no later than exiting O_i . This completes the proof. \square

³The two sides of $uo_1 \dots o_nv$ can be distinguished by the left- and right-hand sides as we move along $uo_1 \dots o_nv$.

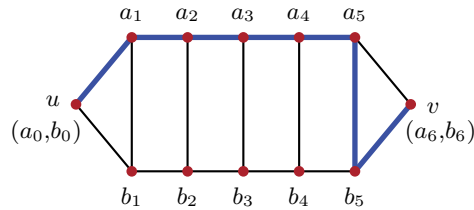
⁴Note that for the purpose of bounding the stretch factor of the Delaunay triangulation, only the case where u, v are unobstructed is relevant. However, for our proof to work, it is necessary to consider the case when u, v are obstructed (see section 4).



(a) Example 1.



(b) Example 2.



(c) Graph representation of Example 2.

FIG. 2. Illustrations for the definitions of $D_{\mathcal{O}}(u, v)$ and $P_{\mathcal{O}}(u, v)$. In both Example 1 and Example 2, $D_{\mathcal{O}}(u, v)$ is the dashed (poly)line, $P_{\mathcal{O}}(u, v)$ is the thick path, and the dotted polyline is the centered polyline between u and v . In Example 1, the terminals u, v are unobstructed, and in Example 2, u, v are obstructed. Figure (c) is the graph representation $\mathbb{G}_{\mathcal{O}}$ of the chain \mathcal{O} in Example 2, where the weight of each edge is the length of the corresponding arc or line segment in \mathcal{O} . The shortest path between u and v in (c) is the thick path $P_{\mathbb{G}_{\mathcal{O}}}(u, v)$, which corresponds to the thick path $P_{\mathcal{O}}(u, v)$ in (b).

DEFINITION 4. We define the shortest path between u and v in \mathcal{O} , denoted by $P_{\mathcal{O}}(u, v)$, to be the shortest path from u to v that consists of arcs in $\{A_1, \dots, A_n\} \cup \{B_1, \dots, B_n\}$ and line segments in $\{\overline{a_1 b_1}, \dots, \overline{a_{n-1} b_{n-1}}\}$. A more formal definition of $P_{\mathcal{O}}(u, v)$ is given below. Consider a weighted graph representation of \mathcal{O} , denoted by $\mathbb{G}_{\mathcal{O}}$, whose vertex set is $\{u = a_0 = b_0\} \cup \{a_1, \dots, a_{n-1}\} \cup \{b_1, \dots, b_{n-1}\} \cup \{v = a_n = b_n\}$ and whose edge set is $\{(a_{i-1}, a_i) \mid 1 \leq i \leq n\} \cup \{(b_{i-1}, b_i) \mid 1 \leq i \leq n\} \cup$

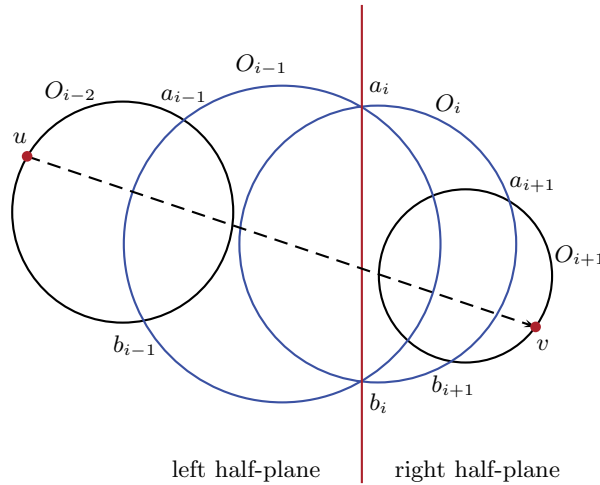


FIG. 3. An illustration for the proof of Proposition 1. The left portion of O_i (w.r.t. $a_i b_i$) is contained in the left portion of O_{i-1} , and the right portion of O_{i-1} is contained in the right portion of O_i .

$\{(a_i, b_i) \mid 1 \leq i \leq n-1\}$. See Figure 2(c) for an illustration. There is a clear bijection between the edge set of $\mathbb{G}_{\mathcal{O}}$ and the set of the arcs and line segments $\{A_1, \dots, A_n\} \cup \{B_1, \dots, B_n\} \cup \{a_1 b_1, \dots, a_{n-1} b_{n-1}\}$ in \mathcal{O} . The weight of any edge in $\mathbb{G}_{\mathcal{O}}$ is the length of the corresponding arc or line segment in \mathcal{O} , that is, $w(a_{i-1}, a_i) = |A_i|$, $w(b_{i-1}, b_i) = |B_i|$, and $w(a_i, b_i) = \|a_i b_i\|$. If an arc or line segment is degenerated, then the weight is 0. Let $P_{\mathbb{G}_{\mathcal{O}}}(u, v)$ be the shortest path between u and v in $\mathbb{G}_{\mathcal{O}}$. Then $P_{\mathcal{O}}(u, v)$ is defined to be the path in \mathcal{O} that corresponds to $P_{\mathbb{G}_{\mathcal{O}}}(u, v)$. The length of $P_{\mathcal{O}}(u, v)$, denoted $|P_{\mathcal{O}}(u, v)|$, is the total weight of the edges in $P_{\mathbb{G}_{\mathcal{O}}}(u, v)$. Refer to Figure 2 for an illustration. Now we can define the stretch factor of a chain \mathcal{O} , denoted by $C_{\mathcal{O}}$, as the maximum value of

$$|P_{\mathcal{O}}(u, v)| / |D_{\mathcal{O}}(u, v)|,$$

over all terminals u, v of \mathcal{O} .

In this paper, we will prove that 1.998 is an upper bound on the stretch factor of the chain.

3. An overview of the proof of Theorem 1. Due to the complex nature of the proof of Theorem 1, in this section we discuss the proof strategy and present an outline of the proof. The main technical details of the proof are captured in two lemmas, whose proofs are given in the subsequent sections.

When \mathcal{O} has only one disk, it is easy to see that for all \mathcal{O}, u , and v , $|P_{\mathcal{O}}(u, v)| / |D_{\mathcal{O}}(u, v)| \leq \pi/2 < \rho$. So it is natural to attempt an inductive proof based on the number of disks in \mathcal{O} . A simple induction would require us to show that adding a disk to a chain will not increase the stretch factor. However, this is not true because one can always increase the stretch factor of a chain by adding a disk to it, albeit by a very small amount [17]. We tackle this problem by amortized analysis. Specifically, we introduce a potential function $\Phi_{\mathcal{O}}$ (to be determined later) and define a target function $\Upsilon_{\mathcal{O}}(u, v)$:

$$(1) \quad \Upsilon_{\mathcal{O}}(u, v) = |P_{\mathcal{O}}(u, v)| - \lambda |D_{\mathcal{O}}(u, v)| + \Phi_{\mathcal{O}},$$

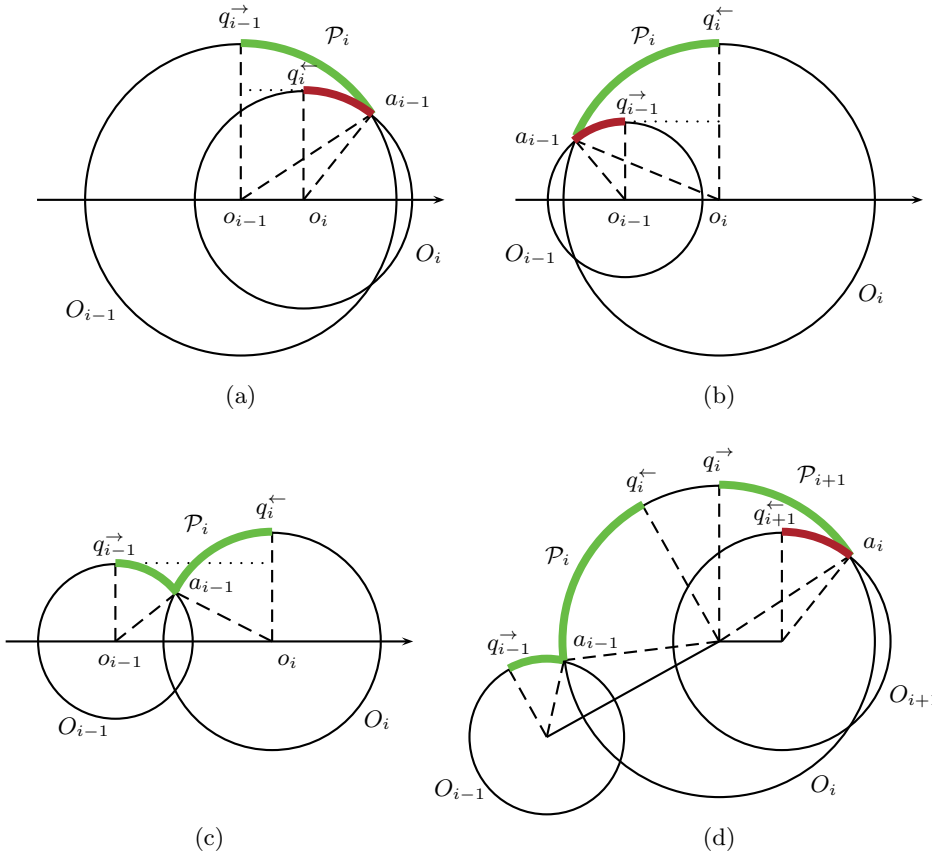


FIG. 4. Illustrations for Definition 5. The path \mathcal{P}_i consists of “heavy” (red or dark gray) arcs and/or “light” (green or light gray) arcs. There are three possible cases for two consecutive disks O_{i-1} and O_i to intersect, as shown in cases (a), (b), and (c). In case (a), Q_{i-1}^{\rightarrow} is light and Q_i^{\leftarrow} is heavy. In this case, $r_{i-1} > r_i$. In case (b), Q_{i-1}^{\rightarrow} is heavy and Q_i^{\leftarrow} is light. In this case, $r_i > r_{i-1}$. In case (c), both Q_{i-1}^{\rightarrow} and Q_i^{\leftarrow} are light. In this case, $r_{i-1} > r_i$, $r_i > r_{i-1}$, and $r_{i-1} = r_i$ are all possible. Figure (d) shows an example of \mathcal{P}_i and \mathcal{P}_{i+1} defined on three consecutive disks O_{i-1}, O_i , and O_{i+1} . Note that O_i has two different peaks. The peak q_i^{\leftarrow} is defined with regard to the preceding disk O_{i-1} . The peak q_i^{\rightarrow} is defined with regard to the succeeding disk O_{i+1} .

where $\lambda = 1.8$ is a parameter whose value is determined by the potential function. Then we will try to prove that $\Upsilon_{\mathcal{O}}(u, v) < 0$ for all \mathcal{O}, u , and v . This is a sufficient condition for Theorem 1, as we will show later in this section.

The key component of the amortized analysis is the selection of an appropriate potential function $\Phi_{\mathcal{O}}$, which is described in the following.

DEFINITION 5. Let O_{i-1} and O_i be two consecutive disks in a chain \mathcal{O} . Without loss of generality, assume that their centers o_{i-1}, o_i lie on a horizontal line and that a_{i-1} is on or above the line $o_{i-1}o_i$. See Figure 4. Let q_{i-1}^{\rightarrow} be the “peak” of O_{i-1} with regard to $o_{i-1}o_i$, i.e., the point on the upper boundary of O_{i-1} that is the farthest from the line $o_{i-1}o_i$. Likewise, let q_i^{\leftarrow} be the “peak” of O_i with regard to $o_{i-1}o_i$ (the sign \rightarrow or \leftarrow indicates whether the peak is defined with the preceding disk or the succeeding disk in \mathcal{O}). Let Q_{i-1}^{\rightarrow} be the upper arc between q_{i-1}^{\rightarrow} and a_{i-1} on the boundary of O_{i-1} and let Q_i^{\leftarrow} be the upper arc between q_i^{\leftarrow} and a_{i-1} on the boundary of O_i . If Q_{i-1}^{\rightarrow} is

inside O_i , we say that it is “heavy” (colored red⁵ in Figure 4); otherwise we say that Q_{i-1}^{\rightarrow} is “light” (colored green⁶ in Figure 4). Likewise, we say that Q_i^{\leftarrow} is “heavy” or “light” depending on whether it is inside O_{i-1} . Let \mathcal{P}_i be a path from q_{i-1}^{\rightarrow} to q_i^{\leftarrow} consisting of Q_{i-1}^{\rightarrow} and Q_i^{\leftarrow} . Let H_i be the horizontal distance traveled along the path \mathcal{P}_i with light arcs contributing positively to H_i and heavy arcs contributing negatively to H_i . Similarly, let V_i be the vertical distance traveled along the path \mathcal{P}_i with light arcs contributing positively to V_i and heavy arcs contributing negatively to V_i . The potential function is defined as follows:

$$(2) \quad \Phi_{\mathcal{O}} = \varphi(r_n - r_1) - \frac{\varphi}{3} \sum_{i=2}^n (2H_i + V_i),$$

where r_i is the radius of O_i and $\varphi = \frac{3}{\sqrt{5}}(1 - \lambda/\rho)$ is a parameter that determines the “weight” of the potential function. When $n = 1$, i.e., when \mathcal{O} has only one disk, $\Phi_{\mathcal{O}} = \varphi(r_1 - r_1) - \frac{\varphi}{3} \sum_{i=2}^1 (2H_i + V_i) = 0$.

The potential function is constructed with three goals in mind, given as three lemmas (Lemmas 1, 2, and 3) in the following. Lemma 1 is easy to prove, but Lemmas 2 and 3 are quite technical and will be proved in subsequent sections.

First goal: the potential function $\Phi_{\mathcal{O}}$ is constructed such that adding a disk to \mathcal{O} does not increase $\Phi_{\mathcal{O}}$, as shown below.

LEMMA 1. $\Phi_{\mathcal{O}} \leq \Phi_{\mathcal{O}_{1,n-1}}$.

Proof. We have the following observations, whose proofs are given in the appendix (section 7.1):

$$(3) \quad H_i = \|o_i o_{i-1}\|,$$

$$(4) \quad V_i \geq |r_i - r_{i-1}|.$$

By the triangle inequality, $\|o_n o_{n-1}\| \geq \|o_n a_{n-1}\| - \|o_{n-1} a_{n-1}\| = r_n - r_{n-1}$. Combining this with (3) and (4), we have

$$(5) \quad \begin{aligned} 2H_n + V_n &\geq 2\|o_n o_{n-1}\| + |r_n - r_{n-1}| \\ &\geq 2(r_n - r_{n-1}) + (r_n - r_{n-1}) \\ &= 3(r_n - r_{n-1}). \end{aligned}$$

Therefore

$$\begin{aligned} \Phi_{\mathcal{O}} - \Phi_{\mathcal{O}_{1,n-1}} &= \left[\varphi(r_n - r_1) - \frac{\varphi}{3} \sum_{i=2}^n (2H_i + V_i) \right] - \left[\varphi(r_{n-1} - r_1) - \frac{\varphi}{3} \sum_{i=2}^{n-1} (2H_i + V_i) \right] \\ &= \varphi(r_n - r_{n-1}) - \frac{\varphi}{3} (2H_n + V_n) \\ &\leq \varphi(r_n - r_{n-1}) - \frac{\varphi}{3} (3(r_n - r_{n-1})) = 0. \quad \square \end{aligned}$$

Second goal: the potential function $\Phi_{\mathcal{O}}$ is constructed such that $\Upsilon_{\mathcal{O}}(u, v) = |P_{\mathcal{O}}(u, v)| - \lambda|D_{\mathcal{O}}(u, v)| + \Phi_{\mathcal{O}} < 0$ for all \mathcal{O}, u , and v , as shown below.

LEMMA 2 (proof in section 4). For all \mathcal{O}, u , and v , $\Upsilon_{\mathcal{O}}(u, v) < 0$.

⁵Red appears as dark gray in black and white print. See electronic version for color images.

⁶Green appears as light gray in black and white print.

Third goal: the potential function $\Phi_{\mathcal{O}}$ is constructed such that its value can be bounded from below as a function of $|P_{\mathcal{O}}(u, v)|$ for some chain \mathcal{O} with certain extremal properties, as shown below.

LEMMA 3 (proof in section 5). *Let \mathbb{O} be a set of chains whose stretch factor is greater than or equal to a threshold τ . If \mathbb{O} is nonempty, then there exists a chain $\mathcal{O}^* \in \mathbb{O}$ with terminals u, v such that $|P_{\mathcal{O}^*}(u, v)|/|D_{\mathcal{O}^*}(u, v)| \geq \tau$ and $\Phi_{\mathcal{O}^*} \geq -\frac{\sqrt{5}\varphi}{3}|P_{\mathcal{O}^*}(u, v)|$.*

Assuming Lemmas 2 and 3 are true, we can prove the main theorem.

Proof for Theorem 1. We will prove that for all \mathcal{O} , the stretch factor $C_{\mathcal{O}}$ is less than $\rho = 1.998$. For the sake of contradiction, suppose that there is a nonempty set \mathbb{O} of chains \mathcal{O} with stretch factor $C_{\mathcal{O}} \geq \rho$. By Lemma 3, there exists a chain $\mathcal{O}^* \in \mathbb{O}$ with terminals u and v such that

$$(6) \quad |P_{\mathcal{O}^*}(u, v)|/|D_{\mathcal{O}^*}(u, v)| \geq \rho$$

and

$$(7) \quad \Phi_{\mathcal{O}^*} \geq -\frac{\sqrt{5}\varphi}{3}|P_{\mathcal{O}^*}(u, v)|.$$

By Lemma 2,

$$(8) \quad \Upsilon_{\mathcal{O}^*}(u, v) = |P_{\mathcal{O}^*}(u, v)| - \lambda|D_{\mathcal{O}^*}(u, v)| + \Phi_{\mathcal{O}^*} < 0.$$

Combining (7) and (8), we have

$$(9) \quad \begin{aligned} & |P_{\mathcal{O}^*}(u, v)| - \lambda|D_{\mathcal{O}^*}(u, v)| - \frac{\sqrt{5}\varphi}{3}|P_{\mathcal{O}^*}(u, v)| \\ & \leq |P_{\mathcal{O}^*}(u, v)| - \lambda|D_{\mathcal{O}^*}(u, v)| + \Phi_{\mathcal{O}^*} \\ & = \Upsilon_{\mathcal{O}^*}(u, v) \\ & < 0. \end{aligned}$$

Recall that $\varphi = \frac{3}{\sqrt{5}}(1 - \lambda/\rho)$. We have

$$(10) \quad \begin{aligned} & |P_{\mathcal{O}^*}(u, v)| - \lambda|D_{\mathcal{O}^*}(u, v)| - \frac{\sqrt{5}\varphi}{3}|P_{\mathcal{O}^*}(u, v)| \\ & = \left(1 - \frac{\sqrt{5}\varphi}{3}\right) |P_{\mathcal{O}^*}(u, v)| - \lambda|D_{\mathcal{O}^*}(u, v)| \\ & = (1 - (1 - \lambda/\rho))|P_{\mathcal{O}^*}(u, v)| - \lambda|D_{\mathcal{O}^*}(u, v)| \\ & = \frac{\lambda}{\rho}|P_{\mathcal{O}^*}(u, v)| - \lambda|D_{\mathcal{O}^*}(u, v)| \\ & = \lambda \left(\frac{|P_{\mathcal{O}^*}(u, v)|}{\rho} - |D_{\mathcal{O}^*}(u, v)| \right). \end{aligned}$$

From (9) and (10), we have $\lambda \left(\frac{|P_{\mathcal{O}^*}(u, v)|}{\rho} - |D_{\mathcal{O}^*}(u, v)| \right) < 0$. In other words, $\frac{|P_{\mathcal{O}^*}(u, v)|}{|D_{\mathcal{O}^*}(u, v)|} < \rho$. This is a contradiction of (6). Therefore \mathbb{O} must be empty and hence $C_{\mathcal{O}} < \rho$ for all \mathcal{O} . \square

As a special case of Theorem 1, we can derive an improved upper bound on the stretch factor of the Delaunay triangulation.

Proof for Corollary 1. We will prove that the stretch factor of a Delaunay triangulation D of a set of points S in the plane is less than $\rho = 1.998$. For any two points $x, y \in S$, let \mathcal{T} be the sequence of triangles in D crossed by the ray \overrightarrow{xy} . Let \mathcal{O} be the corresponding sequence of circumscribed circles of the triangles in \mathcal{T} . It is clear that \mathcal{O} is a chain and x, y are terminals of \mathcal{O} . The shortest path distance from x to y is at most $|P_{\mathcal{O}}(x, y)|$. Since \overrightarrow{xy} stabs through all circles in \mathcal{O} , x, y are unobstructed and hence $|D_{\mathcal{O}}(x, y)| = \|xy\|$. By Theorem 1, the stretch factor of a Delaunay triangulation is at most $|P_{\mathcal{O}}(x, y)|/\|xy\| = |P_{\mathcal{O}}(x, y)|/|D_{\mathcal{O}}(x, y)| < \rho$. \square

The rest of the paper contains the proofs for Lemmas 2 and 3.

4. Proof of Lemma 2. In this section, we will prove that for all \mathcal{O}, u , and v , $\Upsilon_{\mathcal{O}}(u, v) < 0$.

Recall that $\Upsilon_{\mathcal{O}}(u, v) = |P_{\mathcal{O}}(u, v)| - \lambda|D_{\mathcal{O}}(u, v)| + \Phi_{\mathcal{O}}$. Proceed by induction on n , the number of disks in \mathcal{O} . If $n = 1$, then \mathcal{O} has a single disk O_1 . In this case, $\Phi_{\mathcal{O}} = 0$, $P_{\mathcal{O}}(u, v)$ is the shorter arc between u and v on the boundary of O_1 , and $D_{\mathcal{O}}(u, v)$ is the chord between u and v inside O_1 . So $|P_{\mathcal{O}}(u, v)| \leq \pi/2|D_{\mathcal{O}}(u, v)| < 1.8|D_{\mathcal{O}}(u, v)| = \lambda|D_{\mathcal{O}}(u, v)|$ and hence $\Upsilon_{\mathcal{O}}(u, v) = |P_{\mathcal{O}}(u, v)| - \lambda|D_{\mathcal{O}}(u, v)| + \Phi_{\mathcal{O}} = |P_{\mathcal{O}}(u, v)| - \lambda|D_{\mathcal{O}}(u, v)| < 0$ when $n = 1$.

Now assuming that the statement is true when there are less than n disks in \mathcal{O} , where $n \geq 2$, we will prove that it is true when there are n disks in \mathcal{O} .

For the rest of this section, fix an arbitrary chain $\mathcal{O} = (O_1, O_2, \dots, O_n)$ and an arbitrary terminal u on the boundary of O_1 .

Before presenting the technical details of the proof for Lemma 2, we give a road-map of the steps involved in the proof. Essentially, this is a step-by-step process of narrowing down the worst case to a specific configuration where the stretch factor of the chain can be bounded by some smooth single-variant functions, whose values can be easily bounded.

1. First, we eliminate some simple special cases, including the case when $v = a_{n-1}$ or $v = b_{n-1}$ (Proposition 2) and the case when u and v are obstructed (Proposition 3).
2. Then by Propositions 4 and 5 we narrow down the worst case to the condition when v is the ‘‘pivot point’’ on the boundary of O_n , i.e., when the shortest path from u to v including A_n and the the shortest path from u to v including B_n have the same length.
3. Finally we distinguish two cases depending on the angle between uv and $o_{n-1}o_n$. Proposition 6 deals with the case when the angle is large, and Proposition 7 deals with the case when the angle is small, which is by far the most complicated case.

First consider the special case when v is either a_{n-1} or b_{n-1} .

PROPOSITION 2. $\Upsilon_{\mathcal{O}}(u, a_{n-1}) < 0$ and $\Upsilon_{\mathcal{O}}(u, b_{n-1}) < 0$.

Proof. We first prove that $\Upsilon_{\mathcal{O}}(u, a_{n-1}) < 0$. Refer to Figure 5 for an illustration. Consider the subchain $\mathcal{O}_{1,n-1} = (O_1, \dots, O_{n-1})$. Since u, a_{n-1} are terminals of $\mathcal{O}_{1,n-1}$, by the inductive hypothesis,

$$\begin{aligned} & \Upsilon_{\mathcal{O}_{1,n-1}}(u, a_{n-1}) \\ &= |P_{\mathcal{O}_{1,n-1}}(u, a_{n-1})| - \lambda|D_{\mathcal{O}_{1,n-1}}(u, a_{n-1})| + \Phi_{\mathcal{O}_{1,n-1}} \\ (11) \quad &< 0. \end{aligned}$$

We claim that

$$(12) \quad |P_{\mathcal{O}}(u, a_{n-1})| \leq |P_{\mathcal{O}_{1,n-1}}(u, a_{n-1})|$$

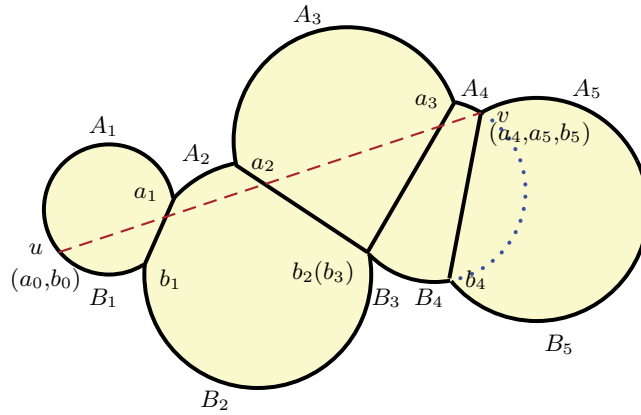


FIG. 5. An illustration for Proposition 2.

and

$$(13) \quad |D_{\mathcal{O}}(u, a_{n-1})| = |D_{\mathcal{O}_{1,n-1}}(u, a_{n-1})|.$$

To verify (12), we note that any arc or line segment in $P_{\mathcal{O}_{1,n-1}}(u, a_{n-1})$ can also be used by $P_{\mathcal{O}}(u, a_{n-1})$, with the exception that the arc B_{n-1} in $\mathcal{O}_{1,n-1}$ between b_{n-1} and a_{n-1} (the dotted arc in Figure 5) is replaced by a “shortcut” in \mathcal{O} via $\overline{b_{n-1}a_{n-1}}$. So clearly $|P_{\mathcal{O}}(u, a_{n-1})| \leq |P_{\mathcal{O}_{1,n-1}}(u, a_{n-1})|$.

Now we verify equality (13). By Definition 3, $D_{\mathcal{O}}(u, a_{n-1})$ is the shortest polyline that consists of line segments $\overline{up_1}, \overline{p_1p_2}, \dots, \overline{p_{n-1}a_{n-1}}$, where $p_i \in \overline{a_i b_i}$ for $1 \leq i \leq n-1$. We can assume $p_{n-1} = a_{n-1}$, because $|\overline{p_{n-2}a_{n-1}}| + |\overline{a_{n-1}a_{n-1}}| = |\overline{p_{n-2}a_{n-1}}| \leq |\overline{p_{n-2}p_{n-1}}| + |\overline{p_{n-1}a_{n-1}}|$ for any p_{n-1} by triangle inequality. So $D_{\mathcal{O}}(u, a_{n-1})$ is the shortest polyline that consists of line segments $\overline{up_1}, \overline{p_1p_2}, \dots, \overline{p_{n-2}a_{n-1}}$ which is the same as $D_{\mathcal{O}_{1,n-1}}(u, a_{n-1})$. Hence $|D_{\mathcal{O}}(u, a_{n-1})| = |D_{\mathcal{O}_{1,n-1}}(u, a_{n-1})|$ and we have equality (13).

From (11), (12), and (13), we have

$$\begin{aligned}
 \Upsilon_{\mathcal{O}}(u, a_{n-1}) &= |P_{\mathcal{O}}(u, a_{n-1})| - \lambda |D_{\mathcal{O}}(u, a_{n-1})| + \Phi_{\mathcal{O}} \\
 &\leq |P_{\mathcal{O}_{1,n-1}}(u, a_{n-1})| - \lambda |D_{\mathcal{O}_{1,n-1}}(u, a_{n-1})| + \Phi_{\mathcal{O}} \\
 &= |P_{\mathcal{O}_{1,n-1}}(u, a_{n-1})| - \lambda |D_{\mathcal{O}_{1,n-1}}(u, a_{n-1})| + \Phi_{\mathcal{O}_{1,n-1}} + \Phi_{\mathcal{O}} - \Phi_{\mathcal{O}_{1,n-1}} \\
 &= \Upsilon_{\mathcal{O}_{1,n-1}}(u, a_{n-1}) + \Phi_{\mathcal{O}} - \Phi_{\mathcal{O}_{1,n-1}} \\
 &< \Phi_{\mathcal{O}} - \Phi_{\mathcal{O}_{1,n-1}} \\
 (14) \quad &\leq 0.
 \end{aligned}$$

The last inequality is from Lemma 1. Similarly, we can prove that $\Upsilon_{\mathcal{O}}(u, b_{n-1}) < 0$. This completes the proof of Proposition 2. \square

Next consider the case when u and v are obstructed. Refer to Figure 6 for an illustration.

PROPOSITION 3. *If u and v are obstructed, then $\Upsilon_{\mathcal{O}}(u, v) < 0$.*

Proof. If u and v are obstructed, then $D_{\mathcal{O}}(u, v)$ contains a point p_j that is either a_j or b_j for some $1 \leq j \leq n-1$. Without loss of generality, assume $p_j = a_j$. Consider two subchains of \mathcal{O} : $\mathcal{O}_{1,j+1} = (O_1, \dots, O_{j+1})$ and $\mathcal{O}_{j+1,n} = (O_{j+1}, \dots, O_n)$. Points

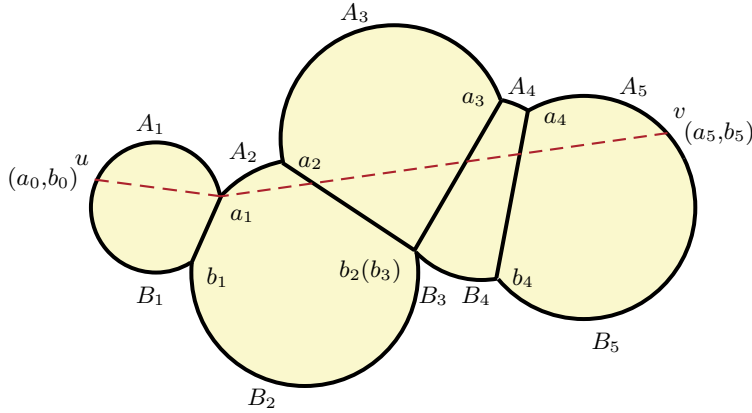


FIG. 6. An illustration for Proposition 3.

u, a_j are terminals of $\mathcal{O}_{1,j+1}$ and points a_j, v are terminals of $\mathcal{O}_{j+1,n}$. If $j = n - 1$, by Proposition 2,

$$(15) \quad \Upsilon_{\mathcal{O}_{1,j+1}}(u, a_j) = \Upsilon_{\mathcal{O}}(u, a_{n-1}) < 0.$$

If $j < n - 1$, $\mathcal{O}_{1,j+1}$ has fewer than n disks, and by the inductive hypothesis

$$(16) \quad \Upsilon_{\mathcal{O}_{1,j+1}}(u, a_j) < 0.$$

On the other hand, $\mathcal{O}_{j+1,n}$ has fewer than n disks, and by the inductive hypothesis,

$$(17) \quad \Upsilon_{\mathcal{O}_{j+1,n}}(a_j, v) < 0.$$

For reasons similar to those for (12) and (13), we have

$$(18) \quad |P_{\mathcal{O}}(u, v)| \leq |P_{\mathcal{O}_{1,j+1}}(u, a_j)| + |P_{\mathcal{O}_{j+1,n}}(a_j, v)|,$$

$$(19) \quad |D_{\mathcal{O}}(u, v)| = |D_{\mathcal{O}_{1,j+1}}(u, a_j)| + |D_{\mathcal{O}_{j+1,n}}(a_j, v)|.$$

Also,

$$\begin{aligned} \Phi_{\mathcal{O}} &= \varphi(r_n - r_1) - \frac{\varphi}{3} \sum_{i=2}^n (2H_i + V_i) \\ &= \varphi(r_n - r_{j+1} + r_{j+1} - r_1) - \frac{\varphi}{3} \sum_{i=2}^{j+1} (2H_i + V_i) - \frac{\varphi}{3} \sum_{i=j+2}^n (2H_i + V_i) \\ &= \varphi(r_{j+1} - r_1) - \frac{\varphi}{3} \sum_{i=2}^{j+1} (2H_i + V_i) + \varphi(r_n - r_{j+1}) - \frac{\varphi}{3} \sum_{i=j+2}^n (2H_i + V_i) \\ (20) \quad &= \Phi_{\mathcal{O}_{1,j+1}} + \Phi_{\mathcal{O}_{j+1,n}}. \end{aligned}$$

Combining (15)–(20), we have

$$\begin{aligned}
 \Upsilon_{\mathcal{O}}(u, v) &= |P_{\mathcal{O}}(u, v)| - \lambda|D_{\mathcal{O}}(u, v)| + \Phi_{\mathcal{O}} \\
 &\leq |P_{\mathcal{O}_{1,j+1}}(u, a_j)| - \lambda|D_{\mathcal{O}_{1,j+1}}(u, a_j)| + \Phi_{\mathcal{O}_{1,j+1}} \\
 &\quad + |P_{\mathcal{O}_{j+1,n}}(a_j, v)| - \lambda|D_{\mathcal{O}_{j+1,n}}(a_j, v)| + \Phi_{\mathcal{O}_{j+1,n}} \\
 &= \Upsilon_{\mathcal{O}_{1,j+1}}(u, a_j) + \Upsilon_{\mathcal{O}_{j+1,n}}(a_j, v) \\
 (21) \quad &< 0,
 \end{aligned}$$

as desired. This completes the proof of Proposition 3. \square

In the rest of the proof for Lemma 2, we assume that u and v are unobstructed, even if it is not explicitly stated. The following definitions are needed. Recall that u is fixed.

DEFINITION 6. Consider the set of terminal points v on O_n such that u and v are unobstructed. Such a set forms an arc (illustrated by the thick arc in Figure 7(a)), denoted by \widehat{A} and referred to as the unobstructed arc.⁷ Denote by $P_{\mathcal{O}}^{A_n}(u, v)$ and $P_{\mathcal{O}}^{B_n}(u, v)$ the shortest paths from u to v that include the arcs A_n and B_n (on the boundary of O_n), respectively. See Figures 7(b) and 7(c) for an illustration. We call v pivotal if $|P_{\mathcal{O}}^{A_n}(u, v)| = |P_{\mathcal{O}}^{B_n}(u, v)|$. Note that \widehat{A} cannot have more than one pivotal point because $|P_{\mathcal{O}}^{A_n}(u, v)| - |P_{\mathcal{O}}^{B_n}(u, v)|$ varies monotonically as v moves along \widehat{A} in one direction.

PROPOSITION 4. If u is fixed and u, v are unobstructed, then the maximum of $\Upsilon_{\mathcal{O}}(u, v)$ occurs when v is an endpoint of \widehat{A} or when v is pivotal in \widehat{A} .

Proof. Let \widehat{A}' be an arbitrary subarc of \widehat{A} that does not contain a pivotal point in its interior. We will use functional analysis to show that the maximum of $\Upsilon_{\mathcal{O}}(u, v)$ for $v \in \widehat{A}'$ occurs when v is an endpoint of \widehat{A}' .

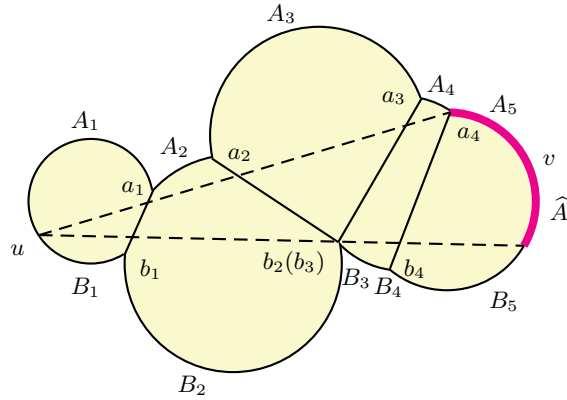
Since \widehat{A}' does not contain a pivotal point in its interior, either $|P_{\mathcal{O}}^{A_n}(u, v)| \leq |P_{\mathcal{O}}^{B_n}(u, v)|$ for every point $v \in \widehat{A}'$ or $|P_{\mathcal{O}}^{B_n}(u, v)| \leq |P_{\mathcal{O}}^{A_n}(u, v)|$ for every point $v \in \widehat{A}'$. Without loss of generality assume that $|P_{\mathcal{O}}^{A_n}(u, v)| \leq |P_{\mathcal{O}}^{B_n}(u, v)|$ for every point v in \widehat{A}' . Fixing other parameters, $\Upsilon_{\mathcal{O}}(u, v)$ is a function of $|A_n|$ as v moves along \widehat{A}' . One observes the following:

1. Since the definition of $\Phi_{\mathcal{O}}$ is independent of v , $\Phi_{\mathcal{O}}$ remains constant when v moves along \widehat{A}' .
2. $|P_{\mathcal{O}}(u, v)|$ is a linear function of $|A_n|$ because $|P_{\mathcal{O}}(u, v)| = \min\{|P_{\mathcal{O}}^{A_n}(u, v)|, |P_{\mathcal{O}}^{B_n}(u, v)|\} = |P_{\mathcal{O}}^{A_n}(u, v)| = |P_{\mathcal{O}}(u, a_{n-1})| + |A_n|$, where $|P_{\mathcal{O}}(u, a_{n-1})|$ remains constant when v moves along \widehat{A}' .
3. $-\lambda|D_{\mathcal{O}}(u, v)|$ is a convex function of $|A_n|$. To see why, refer to Figure 8. Let v_1 be the location of v after $|A_n|$ is increased by an infinitesimal amount (i.e., $d|A_n|$). Then $\overrightarrow{vv_1}$ is tangent to O_n . Let σ be the angle from $\overrightarrow{vv_1}$ to \overrightarrow{uv} . So $\sigma = \pi/2 - \angle uvo_n$. It is a simple geometric observation that

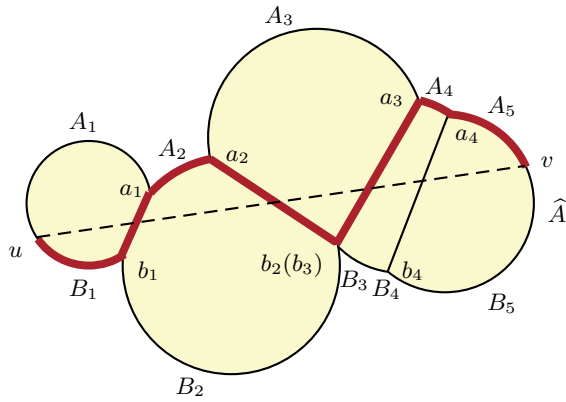
$$(22) \quad \frac{d|D_{\mathcal{O}}(u, v)|}{d|A_n|} = \cos \sigma = \sin(\angle uvo_n).$$

Also observe that $\angle uvo_n$ decreases as v moves away from a_{n-1} along \widehat{A}' and hence $\frac{d\angle uvo_n}{d|A_n|} \leq 0$. Since v is the exit-point of ray \overrightarrow{uv} on O_n , $\angle uvo_n \in$

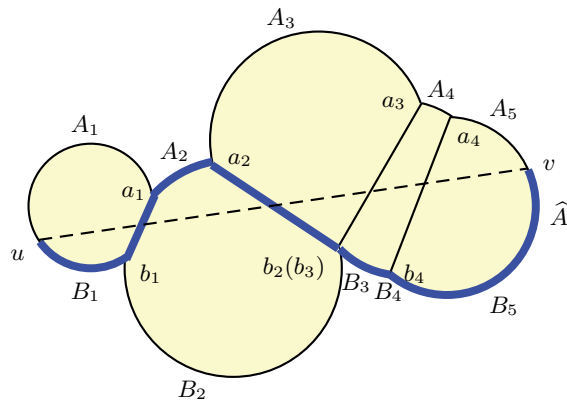
⁷For notational convenience, assume that \widehat{A} includes its endpoints. This makes \widehat{A} a closed set.



(a) The thick arc is the unobstructed arc \hat{A} .



(b) The thick path is $P_{\mathcal{O}}^{A_n}(u, v)$, which is the shortest path from u to v that includes the arcs A_n .



(c) The thick path is $P_{\mathcal{O}}^{B_n}(u, v)$, which is the shortest path from u to v that includes the arcs B_n .

FIG. 7. An illustration for Definition 6. v is pivotal if $|P_{\mathcal{O}}^{A_n}(u, v)| = |P_{\mathcal{O}}^{B_n}(u, v)|$.

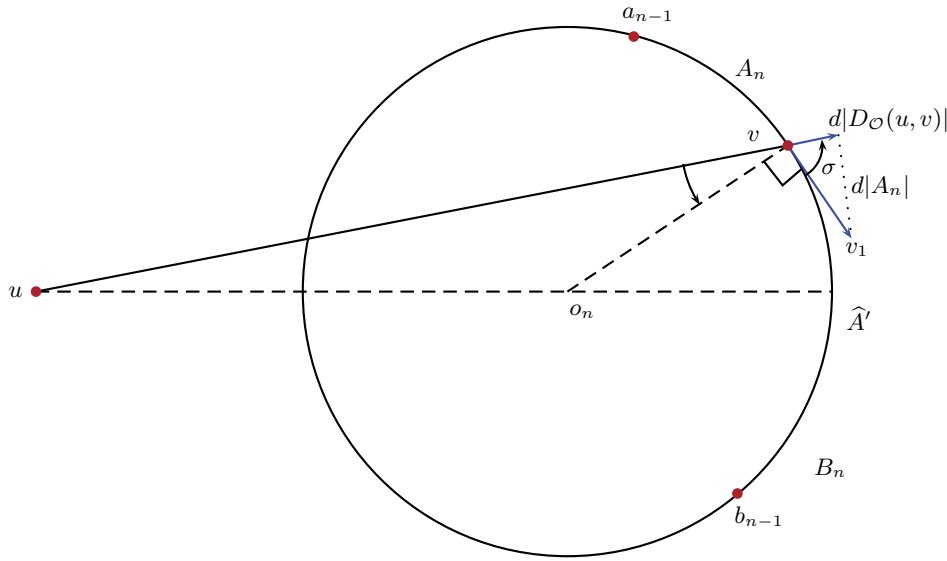


FIG. 8. An illustration for Proposition 4. The angle $\angle uvo_n$ is in the range $(-\pi/2, \pi/2)$. As v moves away from a_{n-1} along \widehat{A}' , $\angle uvo_n$ decreases. When v moves below uo_n , $\angle uvo_n$ becomes negative.

$[-\pi/2, \pi/2]$ and hence $\frac{d \sin(\angle uvo_n)}{d \angle uvo_n} \geq 0$. So

$$(23) \quad \frac{d \sin(\angle uvo_n)}{d|A_n|} = \frac{d \sin(\angle uvo_n)}{d \angle uvo_n} \cdot \frac{d \angle uvo_n}{d|A_n|} \leq 0.$$

Combining (22) and (23), we have

$$\frac{d^2(-\lambda|D_{\mathcal{O}}(u, v)|)}{d|A_n|^2} = -\lambda \cdot \frac{d(\frac{d|D_{\mathcal{O}}(u, v)|}{d|A_n|})}{d|A_n|} = -\lambda \cdot \frac{d(\sin(\angle uvo_n))}{d|A_n|} \geq 0,$$

which implies that $-\lambda|D_{\mathcal{O}}(u, v)|$ is a convex function of $|A_n|$.

Now we know $\Phi_{\mathcal{O}}$, $|P_{\mathcal{O}}(u, v)|$, and $-\lambda|D_{\mathcal{O}}(u, v)|$ are all convex functions of $|A_n|$ (constant and linear functions are also convex). Being a sum of convex functions, $\Upsilon_{\mathcal{O}}(u, v) = |P_{\mathcal{O}}(u, v)| - \lambda|D_{\mathcal{O}}(u, v)| + \Phi_{\mathcal{O}}$ is a convex function of $|A_n|$. This proves that the maximum of $\Upsilon_{\mathcal{O}}(u, v)$ occurs when v is an endpoint of \widehat{A}' . Proposition 4 follows from this, because of the following:

- If \widehat{A} does not contain a pivotal point in its interior, then the maximum of $\Upsilon_{\mathcal{O}}(u, v)$ occurs when v is an endpoint of \widehat{A} and hence Proposition 4 is true.
- If \widehat{A} contains a pivotal point in its interior, we can split \widehat{A} at the pivotal point into two subarcs \widehat{A}_1 and \widehat{A}_2 that do not contain a pivotal point in their interiors. So the maximum of $\Upsilon_{\mathcal{O}}(u, v)$ for all $v \in \widehat{A}_1 \cup \widehat{A}_2$ occurs when v is an endpoint of \widehat{A}_1 or \widehat{A}_2 . The endpoints of \widehat{A}_1 and \widehat{A}_2 are either the pivotal point or the endpoints of \widehat{A} . Thus, Proposition 4 is also true.

This completes the proof of Proposition 4 \square

In the rest of the proof for Lemma 2, we will show that $\Upsilon_{\mathcal{O}}(u, v) < 0$ if v is an endpoint of \widehat{A} and $\Upsilon_{\mathcal{O}}(u, v) < 0$ if v is pivotal. Once these are proven, then by Proposition 4, we have $\Upsilon_{\mathcal{O}}(u, v) < 0$ for any point v in \widehat{A} , which completes the proof of Lemma 2.

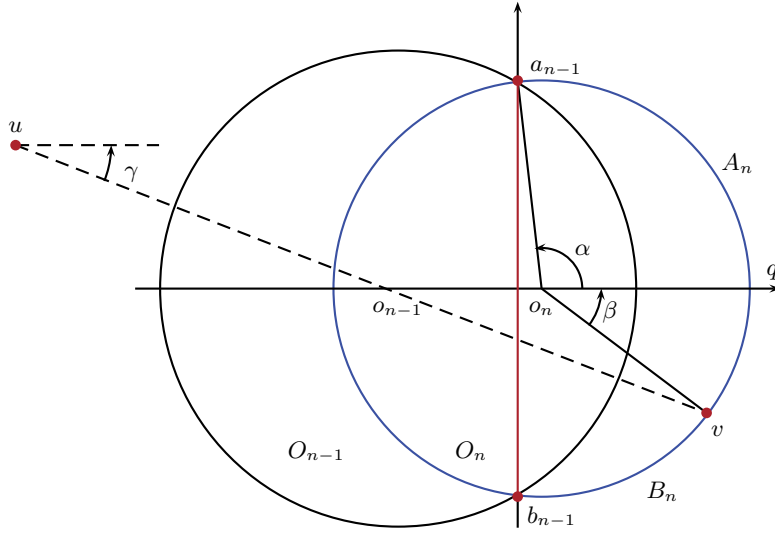


FIG. 9. An illustration of the coordinate system and the definition of the parameters α, β, γ .

PROPOSITION 5. $\Upsilon_{\mathcal{O}}(u, v) < 0$ if v is an endpoint of \hat{A} .

Proof. If v is an endpoint of \hat{A} , then there are two cases: (1) $v \in \{a_{n-1}, b_{n-1}\}$, or (2) u, v are obstructed. See Figure 7 for an illustration. In either case, we have $\Upsilon_{\mathcal{O}}(u, v) < 0$ by Propositions 2 and 3. \square

What remains to be shown is that $\Upsilon_{\mathcal{O}}(u, v) < 0$ when v is pivotal. This requires a careful analysis of the geometry. To start, we fix a coordinate system where the origin is the center point of $\underline{a_{n-1}b_{n-1}}$, the x -axis is $o_{n-1}o_n$, and the y -axis is $a_{n-1}b_{n-1}$. See Figure 9 for an illustration. For any point p in the plane, denote by X_p and Y_p the x - and y -coordinates of p in the coordinate system. By flipping along the x -axis or the y -axis (or both) if necessary, we can assume that $X_{o_{n-1}} \leq X_{o_n}$ (i.e., o_{n-1} is to the left of o_n) and $Y_v \leq Y_u$ (i.e., u is above v). Without loss of generality, let a_{n-1} be above b_{n-1} (the analysis will be similar if b_{n-1} is above a_{n-1}). By Proposition 1, \vec{uv} crosses $\underline{a_{n-1}b_{n-1}}$ from left to right. Hence u is to the left of the y -axis and v is to the right of the y -axis.

Let q be the rightmost intersection between O_n and the x -axis. We define the following parameters. Let $\alpha = \angle qo_n a_{n-1}$ and $\beta = \angle v o_n q$. Let γ be the angle from \vec{uv} to the x -axis in the counterclockwise direction.

The ranges of α, β , and γ are given as follows.

- Since a_{n-1} is on or above the x -axis, $0 \leq \alpha \leq \pi$. If $\alpha = 0$ or $\alpha = \pi$, then $a_{n-1} = b_{n-1}$, which means that $D_{\mathcal{O}}(u, v)$ contains a_{n-1} and $\Upsilon_{\mathcal{O}}(u, v) < 0$ by Proposition 3. So we can assume

$$(24) \quad 0 < \alpha < \pi.$$

- Since v is a pivotal point, we have $|P_{\mathcal{O}}^{A_n}(u, v)| = |P_{\mathcal{O}}^{B_n}(u, v)|$, where $|P_{\mathcal{O}}^{A_n}(u, v)| = |P_{\mathcal{O}}(u, a_{n-1})| + |A_n|$ and $|P_{\mathcal{O}}^{B_n}(u, v)| = |P_{\mathcal{O}}(u, b_{n-1})| + |B_n|$. Thus,

$$(25) \quad |A_n| - |B_n| = |P_{\mathcal{O}}(u, b_{n-1})| - |P_{\mathcal{O}}(u, a_{n-1})|.$$

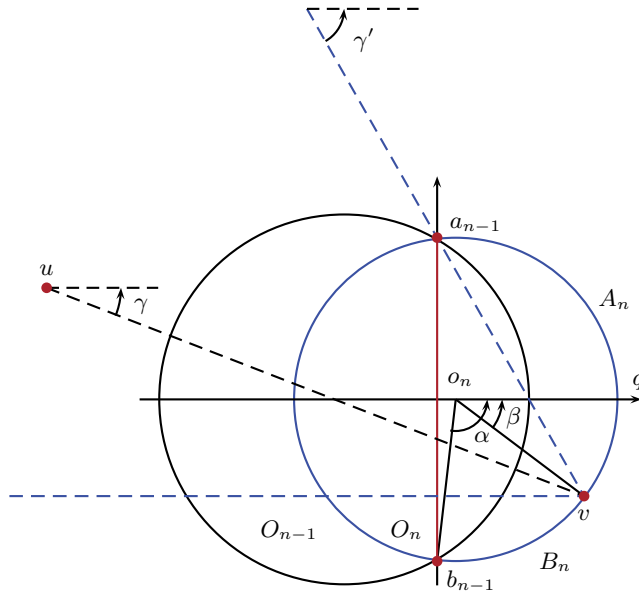


FIG. 10. An illustration for the range of γ . This shows that $0 < \gamma < \gamma'$, where $\gamma' = \pi/2 - \angle b_{n-1}a_{n-1}v = \pi/2 - \frac{\angle b_{n-1}o_nv}{2} = \pi/2 - (\alpha - \beta)/2$.

Since a_{n-1} and b_{n-1} are connected by a line segment $\overline{a_{n-1}b_{n-1}}$, the difference between $|P_{\mathcal{O}}(u, a_{n-1})|$ and $|P_{\mathcal{O}}(u, b_{n-1})|$ is at most $\|\overline{a_{n-1}b_{n-1}}\|$. In other words,

$$(26) \quad -\|\overline{a_{n-1}b_{n-1}}\| \leq |P_{\mathcal{O}}(u, b_{n-1})| - |P_{\mathcal{O}}(u, a_{n-1})| \leq \|\overline{a_{n-1}b_{n-1}}\|.$$

Combining (25) and (26) gives $-\|\overline{a_{n-1}b_{n-1}}\| \leq |A_n| - |B_n| \leq \|\overline{a_{n-1}b_{n-1}}\|$. We further observe that $\|\overline{a_{n-1}b_{n-1}}\| = 2r_n \sin \alpha$ and $|A_n| - |B_n| = 2r_n \beta$. Thus the range of β is

$$(27) \quad -\sin \alpha \leq \beta \leq \sin \alpha.$$

- We have $\gamma \geq 0$ since $Y_v \leq Y_u$.

We claim that the largest value of γ occurs when \overline{uv} passes through a_{n-1} . Here is why. Refer to Figure 10. Since \overline{uv} crosses $\overline{a_{n-1}b_{n-1}}$ and $\gamma \geq 0$, \overline{uv} is sandwiched between the horizontal line passing through v and the line $a_{n-1}v$ (see Figure 10). Within this range, γ obtains its maximum value when \overline{uv} is on the line $a_{n-1}v$, i.e., when \overline{uv} passes through a_{n-1} .

This means $\gamma \leq \pi/2 - \angle b_{n-1}a_{n-1}v = \pi/2 - \frac{\angle b_{n-1}o_nv}{2} = \pi/2 - (\alpha - \beta)/2$ (as illustrated in Figure 10). So the range of γ is

$$(28) \quad 0 \leq \gamma \leq \pi/2 - (\alpha - \beta)/2 < \pi/2.$$

The last inequality is true because from (27) $\alpha - \beta \geq \alpha - \sin \alpha > 0$.

We proceed by distinguishing two cases depending on the value of γ with regard to a threshold value γ^+ , which is defined as

$$(29) \quad \gamma^+ = \frac{3 \sin \alpha - \alpha}{4} + \arcsin \left(\frac{\alpha + \sin \alpha}{4 \lambda \sin(\frac{\alpha + \sin \alpha}{4})} \right).$$

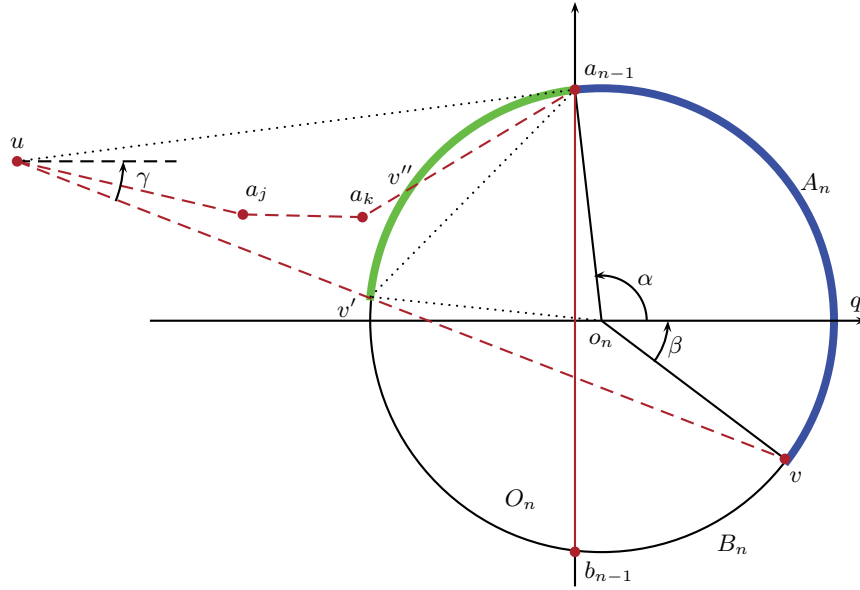


FIG. 11. An illustration for Proposition 6.

PROPOSITION 6. If v is a pivotal point and $\gamma \geq \gamma^+$, then $\Upsilon_{\mathcal{O}}(u, v) < 0$.

Proof. The first step is to show that $|D_{\mathcal{O}}(u, v)| - |D_{\mathcal{O}}(u, a_{n-1})| \geq \|v'v\| - \|v'a_{n-1}\|$, where v' is the entry-point of \vec{uv} on O_n (see Figure 11). This requires a careful verification because in general $D_{\mathcal{O}}(u, a_{n-1})$ may not be a straight line segment.

Recall that u, v are unobstructed. So \vec{uv} crosses all line segments $\overline{a_i b_i}$, $1 \leq i \leq n - 1$, in that order. Visualize $D_{\mathcal{O}}(u, v)$ as a rubber band connecting u and v in Figure 11). As v moves along the boundary of O_n toward a_{n-1} , the line segment $D_{\mathcal{O}}(u, v)$ transforms into a polyline $D_{\mathcal{O}}(u, a_{n-1})$ that “bends” around points $a_j, a_k, \dots \in \{a_1, \dots, a_{n-1}\}$, as illustrated in Figure 11. Therefore $D_{\mathcal{O}}(u, a_{n-1})$ is a path from u to a_{n-1} that is convex-away from ua_{n-1} and is contained in the area bounded by $\overline{ua_{n-1}}$, \overline{uv} , and A_n . Refer to Figure 11. Let a_k be the last turning point in the polyline $D_{\mathcal{O}}(u, a_{n-1})$. So $\overline{a_k a_{n-1}}$ is a part of $D_{\mathcal{O}}(u, a_{n-1})$. By definition, a_k is an intersection between O_k and O_{k+1} . Note that a_k and a_{n-1} are terminals of the subchain $O_{k+1, n}$ and $a_k \neq a_{k+1}$ (otherwise we will choose a_{k+1} as the last turning point). Therefore a_k is the entry-point of $\overline{a_k a_{n-1}}$ on O_{k+1} . By Proposition 1, $\overline{a_k a_{n-1}}$ enters O_{k+1} no later than entering O_n . This means that a_k appears in the ray $\overline{a_k a_{n-1}}$ no later than the entry-point of $\overline{a_k a_{n-1}}$ on O_n , denoted henceforth by v'' . Since $\overline{a_k a_{n-1}}$ is a part of $D_{\mathcal{O}}(u, a_{n-1})$, $\overline{a_k a_{n-1}}$ is contained in the area bounded by $\overline{ua_{n-1}}$, \overline{uv} , and A_n . This means that $\overline{a_k a_{n-1}}$ cannot enter O_n via A_n (the blue⁸ arc in Figure 11). In other words, the entry-point of $\overline{a_k a_{n-1}}$ on O_n (i.e., v'') is on the arc between a_{n-1} and v' (the green⁹ arc in Figure 11). Since a_k appears in $\overline{a_k a_{n-1}}$ no later than v'' , a_k is in $\triangle uv'a_{n-1}$. Now recall that $D_{\mathcal{O}}(u, a_{n-1})$ is a path from u to a_{n-1} that is convex-away from ua_{n-1} . Let

$$\Pi = \overline{ua_{n-1}} \cup D_{\mathcal{O}}(u, a_{n-1}).$$

⁸Blue appears as dark gray in black and white print.

⁹Green appears as light gray in black and white print.

Then Π is a convex polygon. Since Π contains $\overline{a_k a_{n-1}}$ as an edge, the convex polygon Π as a whole is on the same side of the line $a_{n-1}v''$. Combining this with the fact that Π is contained in the area bounded by $\overline{ua_{n-1}}$, \overline{uv} , and A_n , we conclude that Π is contained in the triangle $\Delta uv'a_{n-1}$. See Figure 11 for an illustration. It is known that if a convex polygonal body Π is contained in another convex polygonal body $\Delta uv'a_{n-1}$, then the length of the boundary of Π is less than or equal to the length of the boundary of $\Delta uv'a_{n-1}$ (see [1, p. 42]). Therefore we have $|D_{\mathcal{O}}(u, a_{n-1})| + \|ua_{n-1}\| \leq \|uv'\| + \|v'a_{n-1}\| + \|ua_{n-1}\|$ or, equivalently, $|D_{\mathcal{O}}(u, a_{n-1})| \leq \|uv'\| + \|v'a_{n-1}\|$. Recall that $|D_{\mathcal{O}}(u, v)| = \|uv\|$. We have

$$(30) \quad \begin{aligned} |D_{\mathcal{O}}(u, v)| - |D_{\mathcal{O}}(u, a_{n-1})| &\geq \|uv\| - (\|uv'\| + \|v'a_{n-1}\|) \\ &= \|v'v\| - \|v'a_{n-1}\|, \end{aligned}$$

as claimed in the beginning of this proof.

Again refer to Figure 11. Using simple trigonometric functions, one verifies that $\|v'v\| = 2r_n \cos(\angle vv'o_n)$ and $\|v'a_{n-1}\| = 2r_n \cos(\angle o_nv'a_{n-1})$, where $\angle vv'o_n = \angle o_nv'v = \beta - \gamma$ and $\angle o_nv'a_{n-1} = \angle vv'a_{n-1} - \angle vv'o_n = \frac{\angle vo_na_{n-1}}{2} - \angle vv'o_n = (\alpha + \beta)/2 - (\beta - \gamma) = \alpha/2 - \beta/2 + \gamma$. Combining these with (30) and applying trigonometric identities, we have

$$(31) \quad \begin{aligned} &|D_{\mathcal{O}}(u, v)| - |D_{\mathcal{O}}(u, a_{n-1})| \\ &\geq \|v'v\| - \|v'a_{n-1}\| \\ &= 2r_n \cos(\beta - \gamma) - 2r_n \cos(\alpha/2 - \beta/2 + \gamma) \\ &= -4r_n \sin(\alpha/4 + \beta/4) \sin(3\beta/4 - \alpha/4 - \gamma). \end{aligned}$$

Since v is pivotal, $|P_{\mathcal{O}}(u, v)| = |P_{\mathcal{O}}(u, a_{n-1})| + |A_n| = |P_{\mathcal{O}}(u, b_{n-1})| + |B_n|$. Note that $|A_n| = r_n(\alpha + \beta)$. By Proposition 2, $\Upsilon_{\mathcal{O}}(u, a_{n-1}) = |P_{\mathcal{O}}(u, a_{n-1})| - \lambda|D_{\mathcal{O}}(u, a_{n-1})| + \Phi_{\mathcal{O}} < 0$. Combining these with (31), we have

$$(32) \quad \begin{aligned} \Upsilon_{\mathcal{O}}(u, v) &= |P_{\mathcal{O}}(u, v)| - \lambda|D_{\mathcal{O}}(u, v)| + \Phi_{\mathcal{O}} \\ &= |P_{\mathcal{O}}(u, a_{n-1})| + |A_n| - \lambda|D_{\mathcal{O}}(u, v)| + \Phi_{\mathcal{O}} \\ &= (|P_{\mathcal{O}}(u, a_{n-1})| - \lambda|D_{\mathcal{O}}(u, a_{n-1})| + \Phi_{\mathcal{O}}) \\ &\quad + |A_n| - \lambda|D_{\mathcal{O}}(u, v)| + \lambda|D_{\mathcal{O}}(u, a_{n-1})| \\ &= \Upsilon_{\mathcal{O}}(u, a_{n-1}) + |A_n| - \lambda(|D_{\mathcal{O}}(u, v)| - |D_{\mathcal{O}}(u, a_{n-1})|) \\ &< |A_n| - \lambda(|D_{\mathcal{O}}(u, v)| - |D_{\mathcal{O}}(u, a_{n-1})|) \\ &\leq r_n(\alpha + \beta) + 4\lambda r_n \sin(\alpha/4 + \beta/4) \sin(3\beta/4 - \alpha/4 - \gamma). \end{aligned}$$

Define a function

$$h(\alpha, \beta, \gamma) = r_n(\alpha + \beta) + 4\lambda r_n \sin(\alpha/4 + \beta/4) \sin(3\beta/4 - \alpha/4 - \gamma).$$

Then from (32)

$$(33) \quad \Upsilon_{\mathcal{O}}(u, v) < h(\alpha, \beta, \gamma).$$

We have

$$(34) \quad \frac{\partial h}{\partial \gamma} = -4\lambda r_n \sin(\alpha/4 + \beta/4) \cos(3\beta/4 - \alpha/4 - \gamma).$$

By (27), we have $\alpha/4 + \beta/4 \geq (\alpha - \sin \alpha)/4 > 0$ and $\alpha/4 + \beta/4 \leq (\alpha + \sin \alpha)/4 < \pi/4$. The last inequality is true because $(\alpha + \sin \alpha)/4$ is an increasing function for $\alpha \in (0, \pi)$. So

$$(35) \quad 0 < \alpha/4 + \beta/4 < \pi/4.$$

By (28), we have $3\beta/4 - \alpha/4 - \gamma \geq 3\beta/4 - \alpha/4 - \pi/2 + (\alpha - \beta)/2 = \alpha/4 + \beta/4 - \pi/2 > -\pi/2$. Also $3\beta/4 - \alpha/4 - \gamma < 3\beta/4 \leq (3 \sin \alpha)/4 \leq 3/4$. So

$$(36) \quad -\pi/2 < 3\beta/4 - \alpha/4 - \gamma < 3/4.$$

From (35) and (36), $\sin(\alpha/4 + \beta/4) > 0$ and $\cos(3\beta/4 - \alpha/4 - \gamma) > 0$. Plugging these into (34), we have

$$(37) \quad \frac{\partial h}{\partial \gamma} < 0.$$

Let

$$\gamma^* = 3\beta/4 - \alpha/4 + \arcsin\left(\frac{\alpha + \beta}{4\lambda \sin(\alpha/4 + \beta/4)}\right).$$

It is easy to verify that $h(\alpha, \beta, \gamma^*) = 0$. By a careful calculation that is given in the appendix (section 7.2), we can show that

$$(38) \quad \gamma^* \leq \gamma^+.$$

By (37), h is a decreasing function of γ . So for any $\gamma \geq \gamma^+ \geq \gamma^*$, we have

$$h(\alpha, \beta, \gamma) \leq h(\alpha, \beta, \gamma^+) \leq h(\alpha, \beta, \gamma^*) = 0.$$

Combining this with (33), we have $\Upsilon_{\mathcal{O}}(u, v) < h(\alpha, \beta, \gamma) \leq 0$, as desired. This completes the proof of Proposition 6. \square

The only remaining case is when γ is below the threshold γ^+ .

PROPOSITION 7. *If v is a pivotal point and $\gamma < \gamma^+$, then $\Upsilon_{\mathcal{O}}(u, v) < 0$.*

Proof. Consider the following transformation (see Figure 12):

- Transform O_n by fixing two “anchor” points a_{n-1}, b_{n-1} on its boundary and moving its center o_n along the x -axis toward o_{n-1} , the center of O_{n-1} . During the transformation, the points a_{n-1} and b_{n-1} remain the intersections between the boundaries of O_n and O_{n-1} . The radius of O_n changes during the transformation. In Figure 12, the dotted disks show the process of the transformation.
- Adjust the location of v on the boundary of O_n so that v stays pivotal. In Figure 12, the sequence of large dots shows the locations of v during the transformation.
- Stop the transformation when $\gamma \geq \gamma^+$ or when o_n reaches o_{n-1} .

We will have one of two cases by the end of the transformation: (1) if $\gamma \geq \gamma^+$ at the end of the transformation, then $\Upsilon_{\mathcal{O}}(u, v) < 0$ by Proposition 6; (2) if o_n reaches o_{n-1} at the end of the transformation, then $\Upsilon_{\mathcal{O}}(u, v) = \Upsilon_{\mathcal{O}_{1,n-1}}(u, v) < 0$ by the inductive hypothesis. So in any case, $\Upsilon_{\mathcal{O}}(u, v) < 0$ at the end of the transformation.

In order to prove the proposition, we need to show that $\Upsilon_{\mathcal{O}}(u, v) < 0$ before the transformation. Since $\Upsilon_{\mathcal{O}}(u, v) < 0$ at the end of the transformation, it suffices to

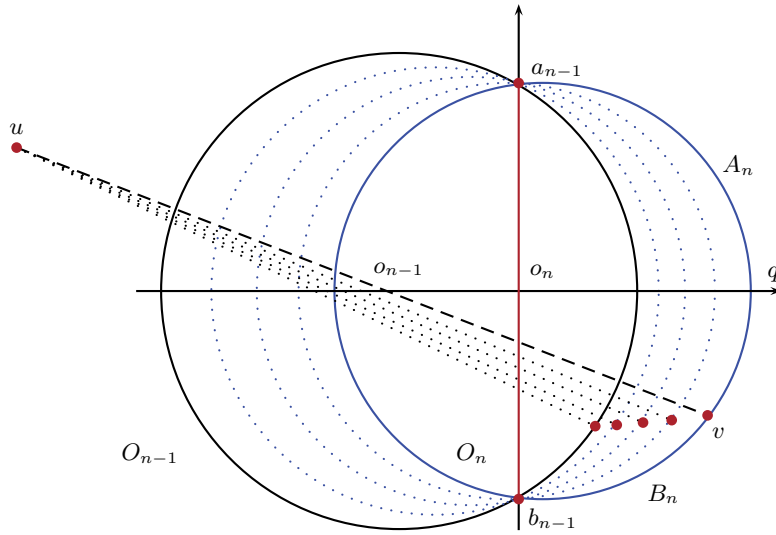


FIG. 12. An illustration for the transformation in Proposition 7. Transform O_n by moving o_n (the center of O_n) toward o_{n-1} (the center of O_{n-1}) along the x -axis while fixing a_{n-1} and b_{n-1} as the intersections between the boundaries of O_n and O_{n-1} . The dotted disks show the process of the transformation. In the transformation, the radius of O_n changes, but v stays pivotal. The large dots show the locations of v during the transformation.

show that $\Upsilon_{\mathcal{O}}(u, v)$ does not decrease during the transformation. Since the transformation is effected by varying X_{o_n} —the x -coordinate of o_n —and X_{o_n} decreases during the transformation, we only need to show that

$$\frac{\partial \Upsilon_{\mathcal{O}}(u, v)}{\partial X_{o_n}} \leq 0$$

during the transformation. We will prove this by analyzing the geometry. Recall that we have fixed a coordinate system where the origin is the center point of $\overline{a_{n-1}b_{n-1}}$, the x -axis is $o_{n-1}o_n$, where o_{n-1} is to the left of o_n , and the y -axis is $a_{n-1}b_{n-1}$, where a_{n-1} is above b_{n-1} .

Since $\Upsilon_{\mathcal{O}}(u, v) = |P_{\mathcal{O}}(u, v)| - \lambda |D_{\mathcal{O}}(u, v)| + \Phi_{\mathcal{O}}$ by (1), we need to calculate the partial derivatives $\frac{\partial |P_{\mathcal{O}}(u, v)|}{\partial X_{o_n}}$, $\frac{\partial \Phi_{\mathcal{O}}}{\partial X_{o_n}}$, and $\frac{\partial |D_{\mathcal{O}}(u, v)|}{\partial X_{o_n}}$. The calculations for them are routine but technical, and are given in the appendix (section 7.3).

$$(39) \quad \frac{\partial |P_{\mathcal{O}}(u, v)|}{\partial X_{o_n}} = \sin \alpha - \alpha \cos \alpha,$$

$$(40) \quad \frac{\partial \Phi_{\mathcal{O}}}{\partial X_{o_n}} = \begin{cases} -\frac{2\varphi}{3} - \frac{4\varphi}{3} \cos \alpha & \text{if } 0 < \alpha < \pi/2, \\ -\frac{2\varphi}{3} - \frac{2\varphi}{3} \cos \alpha & \text{if } \pi/2 \leq \alpha < \pi, \end{cases}$$

$$(41) \quad \frac{\partial |D_{\mathcal{O}}(u, v)|}{\partial X_{o_n}} = \cos \gamma - \cos \alpha (\cos(\beta - \gamma) + \beta \sin(\beta - \gamma)).$$

Based on (41), we define a function

$$(42) \quad f(\alpha, \beta, \gamma) = -\lambda \frac{\partial |D_{\mathcal{O}}(u, v)|}{\partial X_{o_n}}$$

$$(43) \quad = -\lambda (\cos \gamma - \cos \alpha (\cos(\beta - \gamma) + \beta \sin(\beta - \gamma))).$$

We can bound $f(\alpha, \beta, \gamma)$ by single-variant functions in α , as shown in the following inequality, whose proof is quite technical and is given in the appendix (section 7.4):

$$(44) \quad f(\alpha, \beta, \gamma) \leq \begin{cases} \max\{f(\alpha, \sin \alpha, 0), f(\alpha, \sin \alpha, \gamma^+)\} & \text{if } 0 < \alpha < \pi/2, \\ \max\{f(\alpha, 0, 0), f(\alpha, 0, \gamma^+)\} & \text{if } \pi/2 \leq \alpha < \pi. \end{cases}$$

Combining (39), (40), (41), (42), and (44), we have

$$(45) \quad \begin{aligned} \frac{\partial \Upsilon_{\mathcal{O}}(u, v)}{\partial X_{o_n}} &= \frac{\partial |P_{\mathcal{O}}(u, v)|}{\partial X_{o_n}} - \lambda \frac{\partial |D_{\mathcal{O}}(u, v)|}{\partial X_{o_n}} + \frac{\partial |\Phi_{\mathcal{O}}|}{\partial X_{o_n}} \\ &= \frac{\partial |P_{\mathcal{O}}(u, v)|}{\partial X_{o_n}} + f(\alpha, \beta, \gamma) + \frac{\partial |\Phi_{\mathcal{O}}|}{\partial X_{o_n}} \\ &= \begin{cases} \sin \alpha - \alpha \cos \alpha + f(\alpha, \beta, \gamma) - \frac{2\varphi}{3} - \frac{4\varphi}{3} \cos \alpha & \text{if } 0 < \alpha < \pi/2, \\ \sin \alpha - \alpha \cos \alpha + f(\alpha, \beta, \gamma) - \frac{2\varphi}{3} - \frac{2\varphi}{3} \cos \alpha & \text{if } \pi/2 \leq \alpha < \pi \end{cases} \\ &\leq \begin{cases} \sin \alpha - \alpha \cos \alpha + \max\{f(\alpha, \sin \alpha, 0), f(\alpha, \sin \alpha, \gamma^+)\} \\ \quad - \frac{2\varphi}{3} - \frac{4\varphi}{3} \cos \alpha & \text{if } 0 < \alpha < \pi/2, \\ \sin \alpha - \alpha \cos \alpha + \max\{f(\alpha, 0, 0), f(\alpha, 0, \gamma^+)\} \\ \quad - \frac{2\varphi}{3} - \frac{2\varphi}{3} \cos \alpha & \text{if } \pi/2 \leq \alpha < \pi. \end{cases} \end{aligned}$$

By (45), we only need to verify the following four inequalities, where $f(\alpha, \beta, \gamma) = -\lambda(\cos \gamma - \cos \alpha(\cos(\beta - \gamma) + \beta \sin(\beta - \gamma)))$ and $\gamma^+ = \frac{3 \sin \alpha - \alpha}{4} + \arcsin\left(\frac{\alpha + \sin \alpha}{4\lambda \sin(\frac{\alpha + \sin \alpha}{4})}\right)$:

$$(46) \quad g_1(\alpha) = \sin \alpha - \alpha \cos \alpha - \frac{2\varphi}{3} - \frac{2\varphi}{3} \cos \alpha + f(\alpha, 0, 0) < 0, \quad \text{when } \pi/2 \leq \alpha < \pi,$$

$$(47) \quad g_2(\alpha) = \sin \alpha - \alpha \cos \alpha - \frac{2\varphi}{3} - \frac{2\varphi}{3} \cos \alpha + f(\alpha, 0, \gamma^+) < 0, \quad \text{when } \pi/2 \leq \alpha < \pi,$$

$$(48) \quad g_3(\alpha) = \sin \alpha - \alpha \cos \alpha - \frac{2\varphi}{3} - \frac{4\varphi}{3} \cos \alpha + f(\alpha, \sin \alpha, 0) < 0, \quad \text{when } 0 < \alpha < \pi/2,$$

$$(49) \quad g_4(\alpha) = \sin \alpha - \alpha \cos \alpha - \frac{2\varphi}{3} - \frac{4\varphi}{3} \cos \alpha + f(\alpha, \sin \alpha, \gamma^+) < 0, \quad \text{when } 0 < \alpha < \pi/2.$$

Since $g_1, g_2, g_3,$ and g_4 are smooth single-variant functions on small intervals of α , one can easily verify the above inequalities using numerical computing software, such as *Mathematica*. For completeness, a more formal verification is given in the appendix (section 7.5). There we show that $g_1, g_2, g_3,$ and g_4 have small Lipschitz constants, and then use a program that implements a simplified Piyavskii algorithm [16] to verify that their upper bounds are less than 0. This completes the proof of Proposition 7. \square

This is the end of the proof of Lemma 2.

5. Proof of Lemma 3. Let \mathbb{O} be a set of chains whose stretch factor is greater than or equal to a threshold τ . In this section, we will prove that if \mathbb{O} is nonempty, then there exists a chain $\mathcal{O}^* \in \mathbb{O}$ with terminals u, v such that $|P_{\mathcal{O}^*}(u, v)|/|D_{\mathcal{O}^*}(u, v)| \geq \tau$ and $\Phi_{\mathcal{O}^*} \geq -\frac{\sqrt{5}\varphi}{3}|P_{\mathcal{O}^*}(u, v)|$.

Suppose that \mathbb{O} is nonempty. Let \mathbb{E} be the subset of \mathbb{O} consisting of chains in \mathbb{O} with a minimum number of disks. \mathbb{E} is nonempty because \mathbb{O} is nonempty. The number of disks in a chain of \mathbb{E} is denoted n . Next, we will choose a chain \mathcal{O}^* from \mathbb{E} such that the total radii of the disks in \mathcal{O}^* is minimized. We justify below that such an \mathcal{O}^* always exists when \mathbb{E} is nonempty.

Note that the definition of the chain (Definition 1) includes the boundary cases: the case when two consecutive disks are tangent and the case when two connecting arcs of the same disk share an endpoint. Also note that the definition of \mathbb{O} includes the boundary case, i.e., the case when the stretch factor is equal to the threshold τ . Therefore, \mathbb{E} also contains its boundary cases. In other words, \mathbb{E} is a closed set (but \mathbb{E} is not necessarily bounded). Associate with every chain $\mathcal{O} \in \mathbb{E}$ a pair of terminals u, v that yields the worst stretch factor of \mathcal{O} . Every $\mathcal{O} \in \mathbb{E}$ can be represented¹⁰ by a vector $\mathbf{x} \in \mathcal{R}^{3n}$ that specifies, for each of the n disks in \mathcal{O} , its radius and the x - and y -coordinates of its center in a (normalized) coordinate system where u is the origin and v is $(1, 0)$. Therefore \mathbb{E} can be mapped to a nonempty closed set $\mathbb{S} \subseteq \mathcal{R}^{3n}$. Define a function $\mathcal{H} : \mathbb{S} \rightarrow \mathcal{R}$ as $\mathcal{H}(\mathbf{x}) = \sum_{i=1}^n r_i$, where $\mathbf{x} \in \mathbb{S}$ and r_1, \dots, r_n are the radii of the disks in the chain \mathcal{O} represented by \mathbf{x} . $\mathcal{H}(\mathbf{x})$ is a continuous (linear) function on \mathbb{S} . Observe that when the L_2 -norm of \mathbf{x} , $\|\mathbf{x}\|_2$, approaches infinity, the length of the *centered polyline* (the polyline connecting the centers of the disks in \mathcal{O} ; see Definition 2) also approaches infinity. Therefore, to prevent the chain \mathcal{O} from being broken, the total radii of the disks in the chain (i.e., $\mathcal{H}(\mathbf{x})$) must also approach infinity. In other words,

$$\lim_{\|\mathbf{x}\|_2 \rightarrow \infty} \mathcal{H}(\mathbf{x}) \rightarrow \infty.$$

This means that \mathcal{H} is a *coercive* function on \mathbb{S} . It is known that a continuous coercive function on a nonempty closed set $\mathbb{S} \subseteq \mathcal{R}^{3n}$ has a global minimum, regardless of whether \mathbb{S} is bounded or not (see [11, p. 60]). So \mathcal{H} has a global minimum on \mathbb{S} . Therefore we can choose \mathcal{O}^* to be the chain in \mathbb{E} that achieves the global minimum of \mathcal{H} . Let u, v be the terminals associated with \mathcal{O}^* that yield the worst stretch factor. Then \mathcal{O}^* satisfies three conditions:

1. Since $\mathcal{O}^* \in \mathbb{O}$, \mathcal{O}^* has stretch factor $\geq \tau$, i.e., $|P_{\mathcal{O}^*}(u, v)|/|D_{\mathcal{O}^*}(u, v)| \geq \tau$.
2. Since $\mathcal{O}^* \in \mathbb{E}$, the number of disks in \mathcal{O}^* is minimized among all chains in \mathbb{O} .
3. Since \mathcal{O}^* minimizes \mathcal{H} , the sum of the radii $\sum_{\mathcal{O}_i \in \mathcal{O}^*} r_i$ is minimized among all chains in \mathbb{E} .

Because \mathcal{O}^* satisfies conditions 1–3, we can prove that it has the following two properties (Propositions 8 and 9), which may not hold for a general chain.

PROPOSITION 8. *u and v are unobstructed in \mathcal{O}^* .*

Proof. Suppose that $D_{\mathcal{O}^*}(u, v)$ is obstructed. Then $D_{\mathcal{O}^*}(u, v)$ contains a point p_j which is either a_j or b_j for some $1 \leq j \leq n - 1$. Consider two subchains of \mathcal{O}^* : $\mathcal{O}_{1,j}^* = (O_1, \dots, O_j)$ and $\mathcal{O}_{j+1,n}^* = (O_{j+1}, \dots, O_n)$. So u, p_j are terminals of $\mathcal{O}_{1,j}^*$ and p_j, v are terminals of $\mathcal{O}_{j+1,n}^*$. For reasons similar to those for (12) and (13), $|P_{\mathcal{O}^*}(u, v)| \leq |P_{\mathcal{O}_{1,j}^*}(u, p_j)| + |P_{\mathcal{O}_{j+1,n}^*}(p_j, v)|$ and $|D_{\mathcal{O}^*}(u, v)| = |D_{\mathcal{O}_{1,j}^*}(u, p_j)| + |D_{\mathcal{O}_{j+1,n}^*}(p_j, v)|$. Since $|P_{\mathcal{O}^*}(u, v)|/|D_{\mathcal{O}^*}(u, v)| \geq \tau$, we have either $|P_{\mathcal{O}_{1,j}^*}(u, p_j)|/|D_{\mathcal{O}_{1,j}^*}(u, p_j)| \geq \tau$ or $|P_{\mathcal{O}_{j+1,n}^*}(p_j, v)|/|D_{\mathcal{O}_{j+1,n}^*}(p_j, v)| \geq \tau$. This means that either $\mathcal{O}_{1,j}^* \in \mathbb{O}$ or $\mathcal{O}_{j+1,n}^* \in \mathbb{O}$ and both have fewer disks than \mathcal{O}^* —a contradiction of condition 2 of \mathcal{O}^* . So u, v must be unobstructed in \mathcal{O}^* . This completes the proof of Proposition 8. \square

¹⁰Modulo rotating and scaling, which do not affect the stretch factor.

PROPOSITION 9. *Both $A_1A_2 \dots A_n$ and $B_1B_2 \dots B_n$ are shortest paths between u and v in \mathcal{O}^* .*

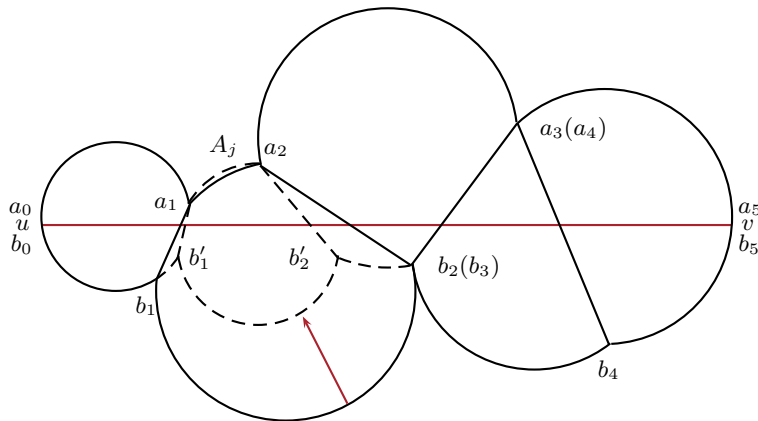
Proof. Suppose that the statement is not true. Then at least one of these two paths, say $B_1B_2 \dots B_n$, is not a shortest path between u and v in \mathcal{O}^* . Let Q be a shortest path between u and v that contains the longest prefix $B_1B_2 \dots B_{j-1}$ of $B_1B_2 \dots B_n$. If $B_1B_2 \dots B_{j-1}$ is empty, then $j = 1$. We have a few observations:

- B_j is not in any shortest path between u and v , because if there is a shortest path Q' that contains B_j , then replacing the subpath of Q' before B_j by $B_1B_2 \dots B_{j-1}$ yields another shortest path Q'' which contains a longer prefix $B_1B_2 \dots B_j$ than Q .
- Since every shortest path between u and v cannot contain B_j , every shortest path between u and v must contain A_j because $\{A_j, B_j\}$ is a cut that separates u and v .
- Since Q contains B_{j-1} and A_j (but not B_j), it must also contain $\overline{a_{j-1}b_{j-1}}$. In the case when $j = 1$, B_0 is degenerated and $a_0 = b_0 = u$.
- B_j is not degenerated because (i) if both A_j and B_j are degenerated, then O_j can be removed from \mathcal{O}^* without changing the stretch factor—a contradiction of condition 2 of \mathcal{O}^* ; (ii) if B_j is degenerated and A_j is not degenerated, then Q can be further shortened by taking $\overline{a_jb_j}$ as a shortcut from b_{j-1} (which equals b_j) to a_j instead of taking $\overline{a_{j-1}b_{j-1}}$ and A_j —a contradiction of the fact that Q is a shortest path.

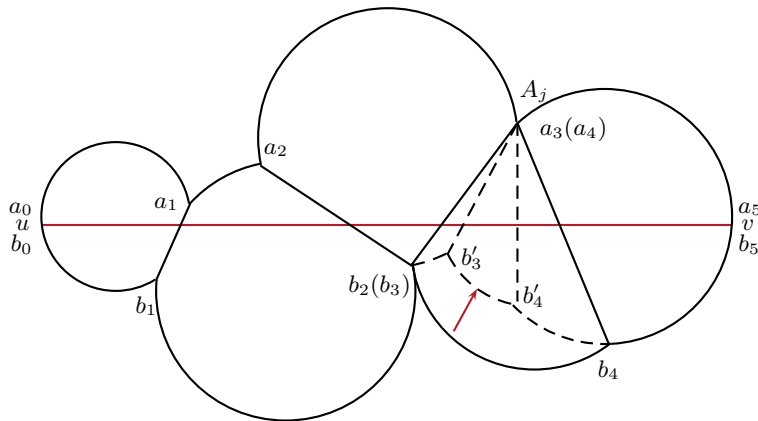
We perform a transformation that shrinks O_j by reducing r_j , as follows: fix a_{j-1} and a_j on the boundary of O_j and reduce O_j 's radius r_j by a small amount; in case where A_j is degenerated, fix a_j (which equals a_{j-1}) on the boundary of O_j and move the center o_j toward a_j by a small amount along the line segment $\overline{o_ja_j}$. See Figure 13 for illustrations. Such transformation can be performed while maintaining the following three properties:

1. \mathcal{O}^* remains a chain. Since a_{j-1} and a_j stay on the boundary of O_j , O_j remains intersected with O_{j-1} and O_{j+1} during the transformation. So property (1) of a chain (in Definition 1) is satisfied. Shrinking O_j will shrink the connecting arcs $C_{j-1}^{(j)}$ and $C_{j+1}^{(j)}$, while $C_{j-1}^{(j-2)}$ and $C_{j+1}^{(j+2)}$ remain the same. Therefore the two connecting arcs on C_{j-1} , namely, $C_{j-1}^{(j-2)}$ and $C_{j-1}^{(j)}$ will not overlap after shrinking O_j . For the same reason, $C_{j+1}^{(j)}$ and $C_{j+1}^{(j+2)}$ will not overlap after shrinking O_j . The only other possible way that property (2) of a chain can be violated is for $C_j^{(j-1)}$ and $C_j^{(j+1)}$ to overlap; but we know that B_j is not degenerated. So shrinking O_j by a sufficiently small amount will not make $C_j^{(j-1)}$ and $C_j^{(j+1)}$ overlap.
2. B_j is still not in any shortest path between u and v . This is because the lengths of the paths between u and v change continuously when O_j shrinks. So we can shrink O_j by a sufficiently small amount such that B_j is still not in any shortest path between u and v .
3. $|D_{\mathcal{O}^*}(u, v)|$ remains unchanged. This is because by Proposition 8, u, v are unobstructed in \mathcal{O}^* . So we can shrink O_j by a sufficiently small amount such that u, v remain unobstructed, which means that $|D_{\mathcal{O}^*}(u, v)| = \|uv\|$ remains the same.

We claim that shrinking O_j by a sufficiently small amount will not decrease $|P_{\mathcal{O}^*}(u, v)|$. We will prove the claim by showing that the length of any shortest path between u and v in \mathcal{O}^* is not decreased after shrinking O_j . Since shrinking O_j



(a) Case 1: A_j is not degenerated.



(b) Case 2: A_j is degenerated.

FIG. 13. Illustrations of Propositions 9: shrinking a disk. There are two cases depending on whether A_j is degenerated.

does not affect \mathcal{O}^* except for A_j and the arcs and line segments containing b_{j-1} or b_j (including B_{j-1} , B_j , B_{j+1} , $a_{j-1}b_{j-1}$, and a_jb_j), we only need to consider the effect of shrinking O_j on shortest paths that contain A_j , b_{j-1} , or b_j .

First consider the effect of shrinking O_j on $|A_j|$. We have $|A_j| \leq |a_{j-1}b_{j-1}| + |B_j| + |a_jb_j|$ because otherwise A_j will not be in a shortest path. Hence $|A_j|$ is less than half of the circumference of O_j . Therefore, shrinking O_j while keeping a_{j-1} and a_j on the boundary of O_j will increase $|A_j|$. For an illustration, see Figure 13(a), which shows that shrinking O_j increases $|A_j|$.

Next consider the effect of shrinking O_j on any shortest path containing b_{j-1} or b_j . Let P be an arbitrary shortest path between u and v in \mathcal{O}^* that contains b_j . Since P contains b_j but not B_j , P includes A_j , a_jb_j , and B_{j+1} . Let b'_j be the new location of b_j after the transformation of O_j (see Figure 13). Then the arc $b_jb'_j$ becomes an extension of B_{j+1} . So after shrinking O_j , $|B_{j+1}|$ becomes $|B_{j+1}| + |b_jb'_j|$ and $|a_jb_j|$

becomes $\|a_j b'_j\|$. Hence, $|P|$ becomes $|P| + |b_j b'_j| + \|a_j b'_j\| - \|a_j b_j\|$ after shrinking O_j . Since $\|a_j b_j\|$ is the shortest distance between a_j and b_j , we have

$$(50) \quad |b_j b'_j| + \|a_j b'_j\| - \|a_j b_j\| > 0.$$

For an illustration, see Figure 13(b), which shows that b'_4 is the new location of b_4 after shrinking O_4 and $|b_4 b'_4| + \|a_4 b'_4\| - \|a_4 b_4\| > 0$. This implies that shrinking O_j increases $|P|$. By a similar argument, shrinking O_j increases the length of any shortest path containing b_{j-1} .

So in any case, shrinking O_j will not decrease $|P_{\mathcal{O}^*}(u, v)|$.

In summary, we have proven that if $B_1 B_2 \dots B_n$ is not a shortest path, then by shrinking a disk $O_j \in \mathcal{O}^*$ we have a new chain that satisfies conditions 1 and 2 of \mathcal{O}^* and has a smaller sum of radii than \mathcal{O}^* , which is a contradiction of condition 3 of \mathcal{O}^* . Therefore the statement of Proposition 9 is true. \square

In order to prove Lemma 3, we then only need to prove the following.

PROPOSITION 10. $\Phi_{\mathcal{O}^*} \geq -\frac{\sqrt{5}\varphi}{3}|P_{\mathcal{O}^*}(u, v)|$.

Proof. Recall that $\Phi_{\mathcal{O}^*} = \varphi(r_n - r_1) - \frac{\varphi}{3} \sum_{i=2}^n (2H_i + V_i)$. Without loss of generality, we can assume that $r_n \geq r_1$, because if this is not the case, we can reverse the labels of the disks in \mathcal{O}^* . So it suffices to show that

$$(51) \quad \sum_{i=2}^n (2H_i + V_i) \leq \sqrt{5}|P_{\mathcal{O}^*}(u, v)|.$$

See Figure 14. We create a chain $\overline{\mathcal{O}^*}$ from \mathcal{O}^* where the centers $o_1 \dots o_n$ are aligned on a straight line, as follows: first rotate O_1 around o_1 such that u comes to a location where $|A_1| = |B_1|$; then rotate O_1 and O_2 as a whole around o_2 such that $|A_2| = |B_2|$; then rotate O_1, O_2 , and O_3 as a whole around o_3 such that $|A_3| = |B_3|$; and so on. $\overline{\mathcal{O}^*}$ is the resulting chain after the rotation operations.

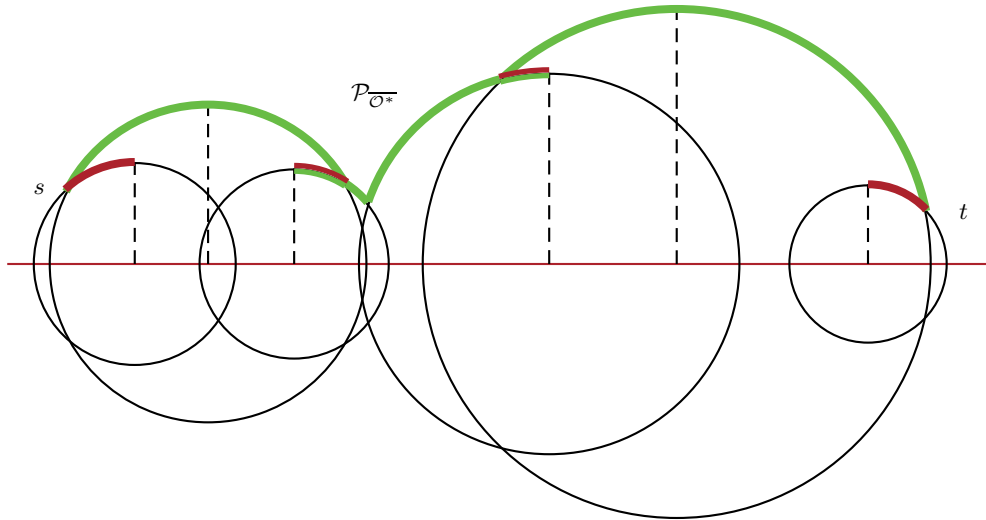


FIG. 14. An illustration for Proposition 10. The centers of the disks in $\overline{\mathcal{O}^*}$ are aligned on a straight line. The path $\mathcal{P}_{\overline{\mathcal{O}^*}}$ consists of “heavy” (red or dark gray) arcs and “light” (green or light gray) arcs. If we let overlapping heavy arcs and light arcs in $\mathcal{P}_{\overline{\mathcal{O}^*}}$ cancel each other out and then remove the heavy arcs at the beginning or the end of $\mathcal{P}_{\overline{\mathcal{O}^*}}$, the resulting path is $\mathcal{P}'_{\overline{\mathcal{O}^*}}$, which is a subpath of $A_1 \dots A_n$ between s and t .

Observe that the rotation operations do not change the total length of the boundary of the chain. So $\sum_{i=1}^n (|A_i| + |B_i|)$ in $\overline{\mathcal{O}^*}$ remains the same as in \mathcal{O}^* , which is $2|P_{\mathcal{O}^*}(u, v)|$ by Proposition 9. In $\overline{\mathcal{O}^*}$, since $A_i = B_i$ for $1 \leq i \leq n$, we have

$$(52) \quad |A_1 \dots A_n| = |B_1 \dots B_n| = |P_{\mathcal{O}^*}(u, v)|.$$

Recall from Definition 5 that H_i and V_i are the horizontal and vertical distances traveled along the path \mathcal{P}_i , where \mathcal{P}_i is a path from q_{i-1}^{\rightarrow} , a peak of O_{i-1} with regard to $o_{i-1}o_i$, to q_i^{\leftarrow} , a peak of O_i with regard to $o_{i-1}o_i$. Also recall that the arcs in \mathcal{P}_i are “light” or “heavy” depending on whether the arc is on the boundary of the chain or not. The light arcs in \mathcal{P}_i contribute positively to H_i and V_i , and the heavy arcs in \mathcal{P}_i contribute negatively to H_i and V_i . Observe that H_i and V_i are determined by the sizes of O_{i-1}, O_i and the distance between them. The rotation operations do not affect the sizes and the distance of O_{i-1} and O_i . So $\sum_{i=2}^n (2H_i + V_i)$ in $\overline{\mathcal{O}^*}$ remains the same as in \mathcal{O}^* .

Since the centers $o_1 \dots o_n$ are all aligned on a straight line in $\overline{\mathcal{O}^*}$, the peaks q_i^{\leftarrow} and q_i^{\rightarrow} of every disk O_i overlap for $2 \leq i \leq n - 1$. So the paths $\mathcal{P}_2, \dots, \mathcal{P}_n$ join at the peaks to form a single path from q_1^{\rightarrow} to q_n^{\leftarrow} ; denote it by $\mathcal{P}_{\overline{\mathcal{O}^*}}$ (see Figure 14). Let $H_{\overline{\mathcal{O}^*}}$ and $V_{\overline{\mathcal{O}^*}}$ denote the horizontal and vertical distances traveled along the path $\mathcal{P}_{\overline{\mathcal{O}^*}}$. Then $H_{\overline{\mathcal{O}^*}} = \sum_{i=2}^n H_i$ and $V_{\overline{\mathcal{O}^*}} = \sum_{i=2}^n V_i$.

We further refine $\mathcal{P}_{\overline{\mathcal{O}^*}}$ into another path $\mathcal{P}'_{\overline{\mathcal{O}^*}}$ as follows (see Figure 14). First we let the overlapping portions of heavy arcs and light arcs in $\mathcal{P}_{\overline{\mathcal{O}^*}}$ cancel each other out; this will not affect $H_{\overline{\mathcal{O}^*}}$ and $V_{\overline{\mathcal{O}^*}}$. All heavy arcs in $\mathcal{P}_{\overline{\mathcal{O}^*}}$ will be canceled in this manner except for those at the beginning or the end of $\mathcal{P}_{\overline{\mathcal{O}^*}}$, which can then be safely removed since they contribute negatively to $H_{\overline{\mathcal{O}^*}}$ and $V_{\overline{\mathcal{O}^*}}$. The resulting path is $\mathcal{P}'_{\overline{\mathcal{O}^*}}$. Let s and t be the endpoints of $\mathcal{P}'_{\overline{\mathcal{O}^*}}$.

Let $H'_{\overline{\mathcal{O}^*}}$ and $V'_{\overline{\mathcal{O}^*}}$ be the horizontal and vertical distances traveled by $\mathcal{P}'_{\overline{\mathcal{O}^*}}$. Then

$$(53) \quad \sum_{i=2}^n H_i = H_{\overline{\mathcal{O}^*}} \leq H'_{\overline{\mathcal{O}^*}}$$

and

$$(54) \quad \sum_{i=2}^n V_i = V_{\overline{\mathcal{O}^*}} \leq V'_{\overline{\mathcal{O}^*}}.$$

Since $\mathcal{P}'_{\overline{\mathcal{O}^*}}$ is a path between s and t , by the generalized triangle inequality, we have

$$(55) \quad \begin{aligned} \sqrt{(H'_{\overline{\mathcal{O}^*}})^2 + (V'_{\overline{\mathcal{O}^*}})^2} &= \sqrt{\left(\int_s^t |dx|\right)^2 + \left(\int_s^t |dy|\right)^2} \\ &\leq \int_s^t \sqrt{(dx)^2 + (dy)^2} \\ &= |\mathcal{P}'_{\overline{\mathcal{O}^*}}|. \end{aligned}$$

Since $\mathcal{P}'_{\overline{\mathcal{O}^*}}$ is a subpath of $A_1 \dots A_n$, from (52), we have

$$(56) \quad |\mathcal{P}'_{\overline{\mathcal{O}^*}}| \leq |A_1 \dots A_n| = |P_{\mathcal{O}^*}(u, v)|.$$

Combining (53), (54), (55), and (56) gives

$$\begin{aligned}
 \sqrt{\left(\sum_{i=2}^n H_i\right)^2 + \left(\sum_{i=2}^n V_i\right)^2} &\leq \sqrt{(H'_{\mathcal{O}^*})^2 + (V'_{\mathcal{O}^*})^2} \\
 &\leq |\mathcal{P}'_{\mathcal{O}^*}| \\
 (57) \qquad \qquad \qquad &\leq |P_{\mathcal{O}^*}(u, v)|.
 \end{aligned}$$

Applying the Cauchy–Schwarz inequality and using (57), we have

$$\begin{aligned}
 2 \sum_{i=2}^n H_i + \sum_{i=2}^n V_i &\leq \sqrt{2^2 + 1^2} \cdot \sqrt{\left(\sum_{i=2}^n H_i\right)^2 + \left(\sum_{i=2}^n V_i\right)^2} \\
 &= \sqrt{5} \cdot \sqrt{\left(\sum_{i=2}^n H_i\right)^2 + \left(\sum_{i=2}^n V_i\right)^2} \\
 (58) \qquad \qquad \qquad &\leq \sqrt{5} \cdot |P_{\mathcal{O}^*}(u, v)|,
 \end{aligned}$$

as required by (51). This proves Proposition 10. □

This completes the proof of Lemma 3.

6. Conclusions. In this paper, we showed that the stretch factor of the Delaunay triangulation is less than 1.998 by proving the same upper bound on the stretch factor of the chain.

There are a few places where our approach can be further improved. First, the potential function can be improved to yield a better upper bound. For example, if we define the potential function $\Phi_{\mathcal{O}}$ to be the length of the segment of \overline{uv} inside O_n , then we can improve the upper bound to 1.98, although the analysis is quite complicated. Second, the key components of our proof are Propositions 6 and 7, whose proofs rely largely on functional analysis. We hope to gain insight of the underlying geometry that will help us simplify the proofs and push the upper bound closer to the tight bound.

7. Appendix.

7.1. Proofs for equality (3) and inequality (4). For this proof, fix a coordinate system where the origin is o_i , the x -axis is $\overrightarrow{o_{i-1}o_i}$, and a_{i-1} is on or above the x -axis. Let $X_{q_{i-1}^{\rightarrow}}$ and $Y_{q_{i-1}^{\rightarrow}}$ be the x - and y -coordinates of q_{i-1}^{\rightarrow} . Let $X_{q_i^{\leftarrow}}$ and $Y_{q_i^{\leftarrow}}$ be the x - and y -coordinates of q_i^{\leftarrow} . Let $X_{a_{i-1}}$ and $Y_{a_{i-1}}$ be the x - and y -coordinates of a_{i-1} . We distinguish three cases.

- *Case 1.* Q_{i-1}^{\rightarrow} is light and Q_i^{\leftarrow} is heavy, as in Figure 4(a). In this case, $r_i < r_{i-1}$, $X_{a_{i-1}} > X_{q_{i-1}^{\rightarrow}}$, and $X_{a_{i-1}} > X_{q_i^{\leftarrow}}$. The horizontal distance traveled by Q_{i-1}^{\rightarrow} and Q_i^{\leftarrow} are $X_{a_{i-1}} - X_{q_{i-1}^{\rightarrow}}$ and $X_{a_{i-1}} - X_{q_i^{\leftarrow}}$, respectively. So

$$H_i = (X_{a_{i-1}} - X_{q_{i-1}^{\rightarrow}}) - (X_{a_{i-1}} - X_{q_i^{\leftarrow}}) = X_{q_i^{\leftarrow}} - X_{q_{i-1}^{\rightarrow}} = \|o_i o_{i-1}\|.$$

In this case, the vertical distance traveled by Q_{i-1}^{\rightarrow} and Q_i^{\leftarrow} are $Y_{q_{i-1}^{\rightarrow}} - Y_{a_{i-1}}$ and $Y_{q_i^{\leftarrow}} - Y_{a_{i-1}}$, respectively (this is the same for all three cases). We have

$$V_i = (Y_{q_{i-1}^{\rightarrow}} - Y_{a_{i-1}}) - (Y_{q_i^{\leftarrow}} - Y_{a_{i-1}}) = Y_{q_{i-1}^{\rightarrow}} - Y_{q_i^{\leftarrow}} = r_{i-1} - r_i = |r_i - r_{i-1}|.$$

- *Case 2.* Q_{i-1}^{\rightarrow} is heavy and Q_i^{\leftarrow} is light, as in Figure 4(b). In this case, $r_i > r_{i-1}$, $X_{q_{i-1}^{\rightarrow}} > X_{a_{i-1}}$, and $X_{q_i^{\leftarrow}} > X_{a_{i-1}}$. The horizontal distance traveled by Q_{i-1}^{\rightarrow} and Q_i^{\leftarrow} are $X_{q_{i-1}^{\rightarrow}} - X_{a_{i-1}}$ and $X_{q_i^{\leftarrow}} - X_{a_{i-1}}$, respectively. So

$$H_i = -(X_{q_{i-1}^{\rightarrow}} - X_{a_{i-1}}) + (X_{q_i^{\leftarrow}} - X_{a_{i-1}}) = X_{q_i^{\leftarrow}} - X_{q_{i-1}^{\rightarrow}} = \|o_i o_{i-1}\|.$$

Same as in Case 1, the vertical distance traveled by Q_{i-1}^{\rightarrow} and Q_i^{\leftarrow} are $Y_{q_{i-1}^{\rightarrow}} - Y_{a_{i-1}}$ and $Y_{q_i^{\leftarrow}} - Y_{a_{i-1}}$, respectively. We have

$$V_i = -(Y_{q_{i-1}^{\rightarrow}} - Y_{a_{i-1}}) + (Y_{q_i^{\leftarrow}} - Y_{a_{i-1}}) = Y_{q_i^{\leftarrow}} - Y_{q_{i-1}^{\rightarrow}} = r_i - r_{i-1} = |r_i - r_{i-1}|.$$

- *Case 3.* Both Q_{i-1}^{\rightarrow} and Q_i^{\leftarrow} are light, as in Figure 4(c). In this case, $X_{a_{i-1}} > X_{q_{i-1}^{\rightarrow}}$ and $X_{q_i^{\leftarrow}} > X_{a_{i-1}}$. The horizontal distance traveled by Q_{i-1}^{\rightarrow} and Q_i^{\leftarrow} are $X_{a_{i-1}} - X_{q_{i-1}^{\rightarrow}}$ and $X_{q_i^{\leftarrow}} - X_{a_{i-1}}$, respectively. So

$$H_i = (X_{a_{i-1}} - X_{q_{i-1}^{\rightarrow}}) + (X_{q_i^{\leftarrow}} - X_{a_{i-1}}) = X_{q_i^{\leftarrow}} - X_{q_{i-1}^{\rightarrow}} = \|o_i o_{i-1}\|.$$

Same as in Case 1, the vertical distance traveled by Q_{i-1}^{\rightarrow} and Q_i^{\leftarrow} are $Y_{q_{i-1}^{\rightarrow}} - Y_{a_{i-1}}$ and $Y_{q_i^{\leftarrow}} - Y_{a_{i-1}}$, respectively. We have

$$V_i = (Y_{q_i^{\leftarrow}} - Y_{a_{i-1}}) + (Y_{q_{i-1}^{\rightarrow}} - Y_{a_{i-1}}).$$

Note that $Y_{q_{i-1}^{\rightarrow}} - Y_{a_{i-1}} \geq 0$ and $Y_{q_i^{\leftarrow}} - Y_{a_{i-1}} \geq 0$. If $r_i \geq r_{i-1}$ (i.e., $Y_{q_i^{\leftarrow}} \geq Y_{q_{i-1}^{\rightarrow}}$), then

$$\begin{aligned} V_i &= (Y_{q_i^{\leftarrow}} - Y_{a_{i-1}}) + (Y_{q_{i-1}^{\rightarrow}} - Y_{a_{i-1}}) \\ &\geq (Y_{q_i^{\leftarrow}} - Y_{a_{i-1}}) - (Y_{q_{i-1}^{\rightarrow}} - Y_{a_{i-1}}) \\ &= Y_{q_i^{\leftarrow}} - Y_{q_{i-1}^{\rightarrow}} \\ &= r_i - r_{i-1} = |r_i - r_{i-1}|. \end{aligned}$$

If $r_i < r_{i-1}$ (i.e., $Y_{q_i^{\leftarrow}} < Y_{q_{i-1}^{\rightarrow}}$), then

$$\begin{aligned} V_i &= (Y_{q_i^{\leftarrow}} - Y_{a_{i-1}}) + (Y_{q_{i-1}^{\rightarrow}} - Y_{a_{i-1}}) \\ &\geq -(Y_{q_i^{\leftarrow}} - Y_{a_{i-1}}) + (Y_{q_{i-1}^{\rightarrow}} - Y_{a_{i-1}}) \\ &= Y_{q_{i-1}^{\rightarrow}} - Y_{q_i^{\leftarrow}} \\ &= r_{i-1} - r_i = |r_i - r_{i-1}|. \end{aligned}$$

- It is impossible for both Q_{i-1}^{\rightarrow} and Q_i^{\leftarrow} to be heavy.

So in any case, $H_i = \|o_i o_{i-1}\|$ and $V_i \geq |r_i - r_{i-1}|$, as required for equality (3) and inequality (4).

7.2. Proof for inequality (38). Recall that

$$\gamma^* = 3\beta/4 - \alpha/4 + \arcsin\left(\frac{\alpha + \beta}{4\lambda \sin(\alpha/4 + \beta/4)}\right).$$

Let $\mu = \alpha/4 + \beta/4$ and $\nu = \frac{\mu}{\lambda \sin \mu} = \frac{\alpha + \beta}{4\lambda \sin(\alpha/4 + \beta/4)}$. So

$$(59) \quad \frac{\partial \mu}{\partial \beta} = \frac{\partial(\alpha/4 + \beta/4)}{\partial \beta} > 0.$$

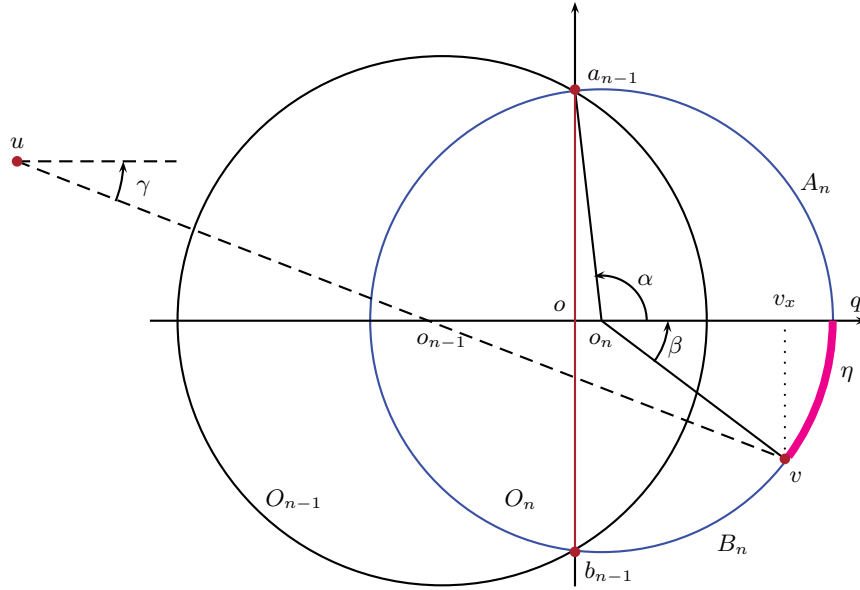


FIG. 15. An illustration for the parameters defined in section 7.3.

By (35), $0 < \mu < \pi/4$. In this range, $\mu < \tan \mu$ and $\sin \mu > 0$. We have

$$(60) \quad \frac{\partial \nu}{\partial \mu} = \frac{\partial \frac{\mu}{\lambda \sin \mu}}{\partial \mu} = (1 - \mu / \tan \mu) / (\lambda \sin \mu) > 0.$$

This means that ν is an increasing function of μ . Therefore $\nu = \frac{\mu}{\lambda \sin \mu} \leq \frac{\pi/4}{\lambda \sin(\pi/4)} < 0.618$. Also $\nu > 0$. In the range $0 < \nu < 0.618$, we have

$$(61) \quad \frac{\partial \arcsin \nu}{\partial \nu} = 1 / \sqrt{1 - \nu^2} > 0.$$

By (59), (60), and (61),

$$\frac{\partial \gamma^*}{\partial \beta} = 3/4 + \frac{\partial \arcsin \nu}{\partial \nu} \cdot \frac{\partial \nu}{\partial \mu} \cdot \frac{\partial \mu}{\partial \beta} > 0.$$

This means γ^* is an increasing function of β , and since $\beta \leq \sin \alpha$, we have

$$\gamma^* \leq \gamma^*|_{\beta=\sin \alpha} = \frac{3 \sin \alpha - \alpha}{4} + \arcsin \left(\frac{\alpha + \sin \alpha}{4 \lambda \sin(\frac{\alpha + \sin \alpha}{4})} \right) = \gamma^+,$$

as required by inequality (38).

7.3. Calculations of the partial derivatives in equalities (39), (40), and (41). First, let's define some parameters (refer to Figure 15 for an illustration):

- Let X_u, Y_u and X_v, Y_v be the x - and y -coordinates of u and v , respectively.
- Let $Y_{a_{n-1}}$ be the y -coordinate of a_{n-1} .
- Let $\eta = \beta r_n$.

We claim that the parameters $X_u, Y_u, Y_{a_{n-1}}$, and η remain constant during the transformation. Here is why. First, X_u and Y_u remain constant during the transformation because the location of u is not changed by the transformation. Second, $Y_{a_{n-1}}$ remains constant during the transformation because a_{n-1} is fixed during the transformation. Third, observe that $\eta = \beta r_n$ is the length of the arc between v and q on the boundary of O_n (the thick arc in Figure 15). Recall that A_n is the arc on the boundary of O_n between a_{n-1} and v , and B_n is the arc on the boundary of O_n between b_{n-1} and v . So $\eta = (|A_n| - |B_n|)/2$. During the transformation, v stays pivotal and hence $|P_{\mathcal{O}}^{A_n}(u, v)| = |P_{\mathcal{O}}^{B_n}(u, v)|$, where $|P_{\mathcal{O}}^{A_n}(u, v)| = |P_{\mathcal{O}}(u, a_{n-1})| + |A_n|$ and $|P_{\mathcal{O}}^{B_n}(u, v)| = |P_{\mathcal{O}}(u, b_{n-1})| + |B_n|$. Therefore, $\eta = (|A_n| - |B_n|)/2 = (|P_{\mathcal{O}}(u, b_{n-1})| - |P_{\mathcal{O}}(u, a_{n-1})|)/2$. Since the transformation does not affect O_1, \dots, O_{n-1} , clearly $|P_{\mathcal{O}}(u, b_{n-1})|$ and $|P_{\mathcal{O}}(u, a_{n-1})|$ remain constant during the transformation. In other words, η remains constant during the transformation.

In what follows, we express all other parameters as functions of $(X_{o_n}, \eta, X_u, Y_u, Y_{a_{n-1}})$ and then calculate their partial derivatives w.r.t. X_{o_n} . This is achievable because, as mentioned above, the parameters η, X_u, Y_u , and $Y_{a_{n-1}}$ are all independent of X_{o_n} .

Refer to Figure 15. Let o be the origin of the coordinate system. Consider the triangle $\triangle o o_n a_{n-1}$. We have $\|o_n a_{n-1}\| = r_n$, $\|o o_n\| = |X_{o_n}|$ ($X_{o_n} < 0$ if o_n is to the left of o and $X_{o_n} \geq 0$ otherwise), and $\|o a_{n-1}\| = Y_{a_{n-1}}$ ($Y_{a_{n-1}}$ is always nonnegative since a_{n-1} is above b_{n-1}). Therefore

$$(62) \quad r_n = \|o_n a_{n-1}\| = \sqrt{\|o o_n\|^2 + \|o a_{n-1}\|^2} = \sqrt{X_{o_n}^2 + Y_{a_{n-1}}^2},$$

and hence

$$(63) \quad \frac{\partial r_n}{\partial X_{o_n}} = \frac{\partial \sqrt{X_{o_n}^2 + Y_{a_{n-1}}^2}}{\partial X_{o_n}} = \frac{2X_{o_n}}{2\sqrt{X_{o_n}^2 + Y_{a_{n-1}}^2}} = \frac{X_{o_n}}{r_n} = -\cos \alpha.$$

The last equality is based on the geometric observation that $\cos \alpha = -\frac{X_{o_n}}{r_n}$ (refer to Figure 15).

Since $\alpha = \pi/2 + \angle o a_{n-1} o_n$ and $\angle o a_{n-1} o_n = \arctan(\frac{X_{o_n}}{Y_{a_{n-1}}})$ (note that $\angle o a_{n-1} o_n \geq 0$ if and only if $X_{o_n} \geq 0$), we have

$$(64) \quad \alpha = \pi/2 + \arctan\left(\frac{X_{o_n}}{Y_{a_{n-1}}}\right),$$

and hence

$$(65) \quad \begin{aligned} \frac{\partial \alpha}{\partial X_{o_n}} &= \frac{\partial(\pi/2 + \arctan(\frac{X_{o_n}}{Y_{a_{n-1}}}))}{\partial X_{o_n}} \\ &= \frac{Y_{a_{n-1}}^2}{X_{o_n}^2 + Y_{a_{n-1}}^2} \cdot \frac{1}{Y_{a_{n-1}}} = \frac{Y_{a_{n-1}}}{X_{o_n}^2 + Y_{a_{n-1}}^2} = \frac{Y_{a_{n-1}}}{r_n^2} = \frac{\sin \alpha}{r_n}. \end{aligned}$$

The last equality is based on the geometric observation that $\sin \alpha = \frac{Y_{a_{n-1}}}{r_n}$ (refer to Figure 15).

Since $\eta = \beta r_n$, we have

$$(66) \quad \beta = \eta/r_n,$$

and hence, from (63), we have

$$(67) \quad \frac{\partial \beta}{\partial X_{o_n}} = \frac{\partial(\eta/r_n)}{\partial X_{o_n}} = -\frac{\eta}{r_n^2} \cdot \frac{\partial r_n}{\partial X_{o_n}} = -\frac{\beta}{r_n} \cdot \frac{\partial r_n}{\partial X_{o_n}} = \frac{\beta \cos \alpha}{r_n}.$$

Refer to Figure 15. Let v_x be the projection of v on the x -axis. Consider the triangle $\Delta_{o_n} v v_x$. We have $X_v - X_{o_n} = ||o_n v|| \cos \beta = r_n \cos \beta$. Therefore

$$(68) \quad X_v = X_{o_n} + r_n \cos \beta,$$

and hence, from (63) and (67), we have

$$(69) \quad \begin{aligned} \frac{\partial X_v}{\partial X_{o_n}} &= \frac{\partial(X_{o_n} + r_n \cos \beta)}{\partial X_{o_n}} = 1 - r_n \sin \beta \frac{\partial \beta}{\partial X_{o_n}} + \cos \beta \frac{\partial r_n}{\partial X_{o_n}} \\ &= 1 - \beta \cos \alpha \sin \beta - \cos \alpha \cos \beta. \end{aligned}$$

Again consider the triangle $\Delta_{o_n} v v_x$. We have

$$(70) \quad Y_v = -||o_n v|| \sin \beta = -r_n \sin \beta,$$

and hence, from (63) and (67), we have

$$(71) \quad \begin{aligned} \frac{\partial Y_v}{\partial X_{o_n}} &= \frac{\partial(-r_n \sin \beta)}{\partial X_{o_n}} = -r_n \cos \beta \frac{\partial \beta}{\partial X_{o_n}} - \sin \beta \frac{\partial r_n}{\partial X_{o_n}} \\ &= -\beta \cos \alpha \cos \beta + \cos \alpha \sin \beta. \end{aligned}$$

Since A_n is the arc on the boundary of O_n between a_{n-1} and v , we have

$$(72) \quad |A_n| = (\alpha + \beta)r_n = \alpha r_n + \beta r_n = \alpha r_n + \eta,$$

and hence, from (63) and (65), we have

$$(73) \quad \frac{\partial |A_n|}{\partial X_{o_n}} = \frac{\partial(\alpha r_n + \eta)}{\partial X_{o_n}} = \frac{\partial(\alpha r_n)}{\partial X_{o_n}} = \alpha \frac{\partial r_n}{\partial X_{o_n}} + r_n \frac{\partial \alpha}{\partial X_{o_n}} = \sin \alpha - \alpha \cos \alpha.$$

Next we will express $\frac{\partial \Upsilon_{\mathcal{O}}(u,v)}{\partial X_{o_n}}$ as a function of α, β , and γ .

By the definition of $\Upsilon_{\mathcal{O}}(u, v)$ (see (1)), we have

$$(74) \quad \begin{aligned} \frac{\partial \Upsilon_{\mathcal{O}}(u, v)}{\partial X_{o_n}} &= \frac{\partial(|P_{\mathcal{O}}(u, v)| - \lambda |D_{\mathcal{O}}(u, v)| + \Phi_{\mathcal{O}})}{\partial X_{o_n}} \\ &= \frac{\partial |P_{\mathcal{O}}(u, v)|}{\partial X_{o_n}} - \lambda \frac{\partial |D_{\mathcal{O}}(u, v)|}{\partial X_{o_n}} + \frac{\partial |\Phi_{\mathcal{O}}|}{\partial X_{o_n}}. \end{aligned}$$

Since v is the pivotal point, we have $|P_{\mathcal{O}}(u, v)| = |P_{\mathcal{O}}(u, a_{n-1})| + |A_n|$, where $|P_{\mathcal{O}}(u, a_{n-1})|$ is independent of X_{o_n} because the transformation does not affect O_1, \dots, O_{n-1} . Hence from (73),

$$(75) \quad \frac{\partial |P_{\mathcal{O}}(u, v)|}{\partial X_{o_n}} = \frac{\partial (P_{\mathcal{O}}(u, a_{n-1}) + |A_n|)}{\partial X_{o_n}} = \frac{\partial |A_n|}{\partial X_{o_n}} = \sin \alpha - \alpha \cos \alpha,$$

which gives equality (39).

From (2),

$$(76) \quad \frac{\partial \Phi_{\mathcal{O}}}{\partial X_{o_n}} = \frac{\partial (\varphi(r_n - r_1) - \frac{\varphi}{3} \sum_{i=2}^{n-1} (2H_i + V_i))}{\partial X_{o_n}}.$$

Since the transformation does not affect O_1, \dots, O_{n-1} , the variables $r_1, H_1, \dots, H_{n-1}, V_1, \dots, V_{n-1}$ are independent of X_{o_n} . We have

$$(77) \quad \begin{aligned} \frac{\partial \Phi_{\mathcal{O}}}{\partial X_{o_n}} &= \frac{\partial (\varphi(r_n - r_1) - \frac{\varphi}{3} \sum_{i=2}^{n-1} (2H_i + V_i))}{\partial X_{o_n}} \\ &= \varphi \frac{\partial r_n}{\partial X_{o_n}} - \frac{\varphi}{3} \left(2 \frac{\partial H_n}{\partial X_{o_n}} + \frac{\partial V_n}{\partial X_{o_n}} \right). \end{aligned}$$

From (3) in section 3, $H_n = ||o_n o_{n-1}|| = X_{o_n} - X_{o_{n-1}}$. Since $X_{o_{n-1}}$ is constant during the transformation,

$$(78) \quad \frac{\partial H_n}{\partial X_{o_n}} = \frac{\partial (X_{o_n} - X_{o_{n-1}})}{\partial X_{o_n}} = \frac{\partial X_{o_n}}{\partial X_{o_n}} = 1.$$

Now let's consider V_n , which is the vertical distance traveled by Q_{n-1}^{\rightarrow} and Q_n^{\leftarrow} , with light arcs contributing positively and heavy arcs contributing negatively (refer to Figure 4). The vertical distance traveled by Q_n^{\leftarrow} is $r_n - Y_{a_{n-1}}$, and the vertical distance traveled by Q_{n-1}^{\rightarrow} is $r_{n-1} - Y_{a_{n-1}}$.

When $0 < \alpha < \pi/2$ (as in case (a) of Figure 4), Q_{n-1}^{\rightarrow} is light and Q_n^{\leftarrow} is heavy. So $V_n = (r_{n-1} - Y_{a_{n-1}}) - (r_n - Y_{a_{n-1}}) = r_{n-1} - r_n$. Since r_{n-1} is constant during the transformation,

$$(79) \quad \frac{\partial V_n}{\partial X_{o_n}} = \frac{\partial (r_{n-1} - r_n)}{\partial X_{o_n}} = -\frac{\partial r_n}{\partial X_{o_n}} = \cos \alpha.$$

When $\pi/2 \leq \alpha < \pi$, there are two possibilities: (1) Q_n^{\leftarrow} is light and Q_{n-1}^{\rightarrow} is heavy (as in case (b) of Figure 4), and $V_n = -(r_{n-1} - Y_{a_{n-1}}) + (r_n - Y_{a_{n-1}}) = r_n - r_{n-1}$. Since r_{n-1} is constant during the transformation,

$$(80) \quad \frac{\partial V_n}{\partial X_{o_n}} = \frac{\partial (r_n - r_{n-1})}{\partial X_{o_n}} = \frac{\partial r_n}{\partial X_{o_n}} = -\cos \alpha.$$

(2) Q_n^{\leftarrow} and Q_{n-1}^{\rightarrow} are both light (as in case (c) of Figure 4), and $V_n = (r_{n-1} - Y_{a_{n-1}}) + (r_n - Y_{a_{n-1}}) = r_n + r_{n-1} - 2Y_{a_{n-1}}$. Since r_{n-1} and $Y_{a_{n-1}}$ are constant during the

transformation,

$$(81) \quad \frac{\partial V_n}{\partial X_{o_n}} = \frac{\partial(r_n + r_{n-1} - 2Y_{a_{n-1}})}{\partial X_{o_n}} = \frac{\partial r_n}{\partial X_{o_n}} = -\cos \alpha.$$

Therefore, combining (63), (78), (79), (80), and (81), we have

$$(82) \quad \begin{aligned} \frac{\partial \Phi_{\mathcal{O}}}{\partial X_{o_n}} &= \frac{\partial(\varphi(r_n - r_1) - \frac{\varphi}{3} \sum_{i=2}^{n-1} (2H_i + V_i))}{\partial X_{o_n}} \\ &= \varphi \frac{\partial r_n}{\partial X_{o_n}} - \frac{\varphi}{3} \left(2 \frac{\partial H_n}{\partial X_{o_n}} + \frac{\partial V_n}{\partial X_{o_n}} \right) \\ &= \begin{cases} -\varphi \cos \alpha - \frac{2\varphi}{3} - \frac{\varphi}{3} \cos \alpha & \text{if } 0 < \alpha < \pi/2, \\ -\varphi \cos \alpha - \frac{2\varphi}{3} + \frac{\varphi}{3} \cos \alpha & \text{if } \pi/2 \leq \alpha < \pi, \end{cases} \\ &= \begin{cases} -\frac{2\varphi}{3} - \frac{4\varphi}{3} \cos \alpha & \text{if } 0 < \alpha < \pi/2, \\ -\frac{2\varphi}{3} - \frac{2\varphi}{3} \cos \alpha & \text{if } \pi/2 \leq \alpha < \pi, \end{cases} \end{aligned}$$

which gives equality (40).

For the case under consideration, $|D_{\mathcal{O}}(u, v)| = \|uv\|$ and hence

$$(83) \quad \begin{aligned} \frac{\partial |D_{\mathcal{O}}(u, v)|}{\partial X_{o_n}} &= \frac{\partial \|uv\|}{\partial X_{o_n}} = \frac{\partial \sqrt{(X_v - X_u)^2 + (Y_v - Y_u)^2}}{\partial X_{o_n}} \\ &= \frac{X_v - X_u}{\sqrt{(X_v - X_u)^2 + (Y_v - Y_u)^2}} \cdot \frac{\partial (X_v - X_u)}{\partial X_{o_n}} \\ &\quad + \frac{Y_v - Y_u}{\sqrt{(X_v - X_u)^2 + (Y_v - Y_u)^2}} \cdot \frac{\partial (Y_v - Y_u)}{\partial X_{o_n}} \\ &= \frac{X_v - X_u}{\|uv\|} \cdot \frac{\partial (X_v - X_u)}{\partial X_{o_n}} + \frac{Y_v - Y_u}{\|uv\|} \cdot \frac{\partial (Y_v - Y_u)}{\partial X_{o_n}} \\ &= \cos \gamma \frac{\partial X_v}{\partial X_{o_n}} - \sin \gamma \frac{\partial Y_v}{\partial X_{o_n}}. \end{aligned}$$

The last equality is true because $\cos \gamma = \frac{X_v - X_u}{\|uv\|}$, $-\sin \gamma = \frac{Y_v - Y_u}{\|uv\|}$, and X_u, Y_u are independent of X_{o_n} .

Combining (69), (71), and (83) and by the trigonometric identities, we have

$$(84) \quad \begin{aligned} \frac{\partial |D_{\mathcal{O}}(u, v)|}{\partial X_{o_n}} &= \cos \gamma \frac{\partial X_v}{\partial X_{o_n}} - \sin \gamma \frac{\partial Y_v}{\partial X_{o_n}} \\ &= \cos \gamma (1 - \beta \cos \alpha \sin \beta - \cos \alpha \cos \beta) \\ &\quad - \sin \gamma (-\beta \cos \alpha \cos \beta + \cos \alpha \sin \beta) \\ &= \cos \gamma - \cos \alpha (\beta \sin \beta \cos \gamma - \beta \cos \beta \sin \gamma + \cos \beta \cos \gamma + \sin \beta \sin \gamma) \\ (85) \quad &= \cos \gamma - \cos \alpha (\cos(\beta - \gamma) + \beta \sin(\beta - \gamma)), \end{aligned}$$

which gives equality (41).

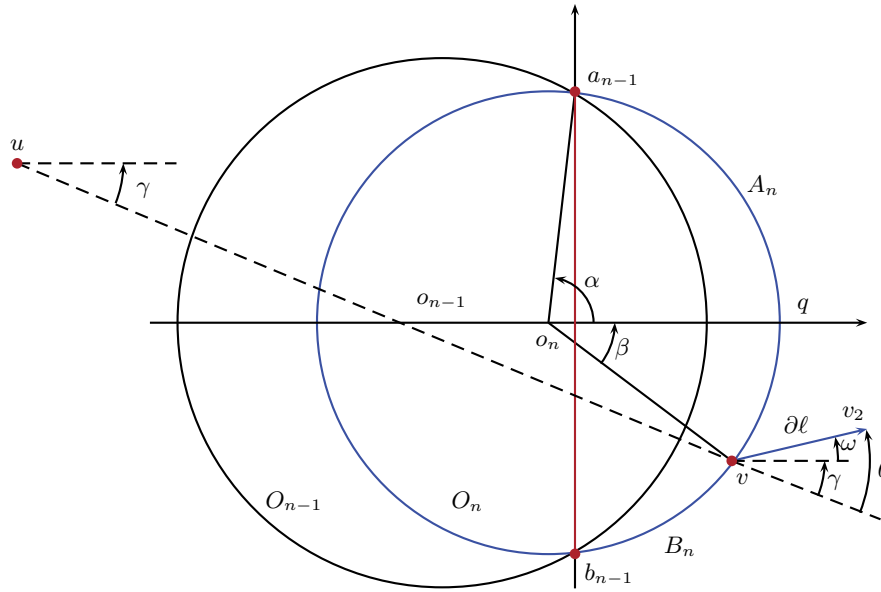


FIG. 16. An illustration for the definition of θ and ω .

7.4. Proof for inequality (44). Recall that by definition

$$(86) \quad f(\alpha, \beta, \gamma) = -\lambda \frac{\partial |D_{\mathcal{O}}(u, v)|}{\partial X_{o_n}}$$

$$(87) \quad = -\lambda(\cos \gamma - \cos \alpha(\cos(\beta - \gamma) + \beta \sin(\beta - \gamma))),$$

where $\lambda = 1.8$ is a constant.

We will first analyze the occurrence of the maximum value of $f(\alpha, \beta, \gamma)$ w.r.t. γ . Let v_2 be the location of v when X_{o_n} increases by ∂X_{o_n} (i.e., o_n moves to the right by ∂X_{o_n}).¹¹ Let $\partial \ell$ be the distance from v to v_2 . Let ω be the angle from the x -axis to $\overrightarrow{vv_2}$. See Figure 16 for an illustration.¹² So

$$(88) \quad \cos \omega = \frac{\partial X_v}{\partial \ell}$$

and

$$(89) \quad \sin \omega = \frac{\partial Y_v}{\partial \ell},$$

where X_v and Y_v are the x - and y -coordinates of v . Recall that γ is the angle from \overrightarrow{uv} to the x -axis. Let $\theta = \omega + \gamma$.

¹¹Note that here o_n is moving in the opposite direction to the transformation of O_n defined in the beginning of the proof for Proposition 7. While it is necessary for the correctness of the proof to move o_n toward o_{n-1} when defining the transformation of O_n , here we move o_n away from o_{n-1} to be consistent with the sign of ∂X_{o_n} for the sake of notational convenience.

¹²In Figure 16, both $\partial \ell$ and ω are exaggerated for illustrative purposes.

From (83), (88), and (89) we have

$$\begin{aligned}
 \frac{\partial |D_{\mathcal{O}}(u, v)|}{\partial X_{o_n}} &= \cos \gamma \frac{\partial X_v}{\partial X_{o_n}} - \sin \gamma \frac{\partial Y_v}{\partial X_{o_n}} \\
 &= \left(\cos \gamma \frac{\partial X_v}{\partial \ell} - \sin \gamma \frac{\partial Y_v}{\partial \ell} \right) \frac{\partial \ell}{\partial X_{o_n}} \\
 &= (\cos \gamma \cos \omega - \sin \gamma \sin \omega) \frac{\partial \ell}{\partial X_{o_n}} \\
 &= \cos(\omega + \gamma) \frac{\partial \ell}{\partial X_{o_n}} \\
 (90) \qquad &= \cos \theta \frac{\partial \ell}{\partial X_{o_n}}.
 \end{aligned}$$

Therefore, from (42) and (90), $f = -\lambda \frac{\partial |D_{\mathcal{O}}(u, v)|}{\partial X_{o_n}} = -\lambda \cos \theta \frac{\partial \ell}{\partial X_{o_n}}$. Recall that $\partial \ell$ was defined to be $\|v v_2\|$, where v_2 is the location of v when X_{o_n} increases by ∂X_{o_n} . Hence $\frac{\partial \ell}{\partial X_{o_n}} > 0$. Also note that $\frac{\partial \ell}{\partial X_{o_n}}$ is determined by α and β . In other words, $\frac{\partial \ell}{\partial X_{o_n}}$ is independent of γ . Therefore, with α and β fixed, $f(\alpha, \beta, \gamma)$ is maximized when $\cos \theta$ is minimized, i.e., when θ is minimized or maximized for $\theta \in [-\pi, \pi]$. Since $\theta = \omega + \gamma$, where ω is independent of γ , θ is minimized when $\gamma = 0$ and is maximized when $\gamma = \gamma^+$. Therefore the maximum of f occurs when $\gamma = 0$ or when $\gamma = \gamma^+$. In other words,

$$(91) \qquad f(\alpha, \beta, \gamma) \leq \max\{f(\alpha, \beta, 0), f(\alpha, \beta, \gamma^+)\},$$

where $\gamma^+ = \frac{3 \sin \alpha - \alpha}{4} + \arcsin\left(\frac{\alpha + \sin \alpha}{4 \lambda \sin(\frac{\alpha + \sin \alpha}{4})}\right)$.

We then analyze the occurrence of the maximum value of $f(\alpha, \beta, \gamma)$ w.r.t. β . We have

$$\begin{aligned}
 \frac{\partial f}{\partial \beta} &= \frac{\partial(-\lambda(\cos \gamma - \cos \alpha(\cos(\beta - \gamma) + \beta \sin(\beta - \gamma))))}{\partial \beta} \\
 &= -\lambda \frac{\partial(\cos \gamma - \cos \alpha(\cos(\beta - \gamma) + \beta \sin(\beta - \gamma)))}{\partial \beta} \\
 &= \lambda \cos \alpha \frac{\partial(\cos(\beta - \gamma) + \beta \sin(\beta - \gamma))}{\partial \beta} \\
 &= \lambda \cos \alpha (-\sin(\beta - \gamma) + \sin(\beta - \gamma) + \beta \cos(\beta - \gamma)) \\
 &= \lambda \beta \cos \alpha \cos(\beta - \gamma),
 \end{aligned}$$

where $\beta - \gamma = \angle o_n v u$. Since v is the exit-point of $\vec{u \hat{v}}$ on the boundary of O_n , the angle $\angle o_n v u$ is in the range $[-\pi/2, \pi/2]$. In other words, $-\pi/2 \leq \beta - \gamma \leq \pi/2$ and hence $\cos(\beta - \gamma) \geq 0$. We distinguish two cases:

1. $\pi/2 \leq \alpha < \pi$. In this case, $\cos \alpha \leq 0$. Since $\cos(\beta - \gamma) \geq 0$, we have $\frac{\partial f}{\partial \beta} = \lambda \beta \cos \alpha \cos(\beta - \gamma) \leq 0$ when $\beta \geq 0$, and $\frac{\partial f}{\partial \beta} \geq 0$ when $\beta \leq 0$. This means that f is a nondecreasing function of β when $\beta \leq 0$ and a nonincreasing function of β when $\beta \geq 0$. So f obtains its maximum value when $\beta = 0$, i.e.,

$$(92) \qquad f(\alpha, \beta, \gamma) \leq f(\alpha, 0, \gamma).$$

2. $0 < \alpha < \pi/2$. In this case, $\cos \alpha \geq 0$. Since $\cos(\beta - \gamma) \geq 0$, we have $\frac{\partial f}{\partial \beta} = \lambda \beta \cos \alpha \cos(\beta - \gamma) \geq 0$ when $\beta \geq 0$, and $\frac{\partial f}{\partial \beta} \leq 0$ when $\beta \leq 0$. From (43), we have

(93)

$$\begin{aligned}
 & f(\alpha, \beta, \gamma) - f(\alpha, -\beta, \gamma) \\
 &= -\lambda(\cos \gamma - \cos \alpha(\cos(\beta - \gamma) + \beta \sin(\beta - \gamma))) \\
 &\quad + \lambda(\cos \gamma - \cos \alpha(\cos(-\beta - \gamma) - \beta \sin(-\beta - \gamma))) \\
 &= \lambda \cos \alpha[(\cos(\beta - \gamma) + \beta \sin(\beta - \gamma)) - (\cos(-\beta - \gamma) - \beta \sin(-\beta - \gamma))] \\
 &= \lambda \cos \alpha[\cos(\beta - \gamma) + \beta \sin(\beta - \gamma) - \cos(\beta + \gamma) - \beta \sin(\beta + \gamma)] \\
 &= \lambda \cos \alpha[\cos(\beta - \gamma) - \cos(\beta + \gamma) + \beta \sin(\beta - \gamma) - \beta \sin(\beta + \gamma)] \\
 &= \lambda \cos \alpha[-2 \sin \beta \sin(-\gamma) + 2\beta \cos \beta \sin(-\gamma)] \\
 &\quad \text{(by trigonometric identities)} \\
 &= \lambda \cos \alpha[2 \sin \beta \sin \gamma - 2\beta \cos \beta \sin \gamma] \\
 &= 2\lambda \cos \alpha \sin \gamma(\sin \beta - \beta \cos \beta).
 \end{aligned}$$

Recall that $\cos \alpha \geq 0$. By (28), $0 \leq \gamma < \pi/2$ and hence $\sin \gamma \geq 0$. By (27), $\beta \leq \sin \alpha \leq 1$. If $\beta \geq 0$, then $0 \leq \beta \leq 1$, and within this range, one verifies that $\sin \beta - \beta \cos \beta \geq 0$. So when $\beta \geq 0$, we have $f(\alpha, \beta, \gamma) - f(\alpha, -\beta, \gamma) \geq 0$. In other words,

$$(94) \quad f(\alpha, \beta, \gamma) \leq f(\alpha, |\beta|, \gamma).$$

As mentioned in the beginning of this case, we have $\frac{\partial f}{\partial \beta} \geq 0$ for $\beta \geq 0$, and from (27), $0 \leq |\beta| \leq \sin \alpha$. Hence, we have

$$(95) \quad f(\alpha, |\beta|, \gamma) \leq f(\alpha, \sin \alpha, \gamma).$$

From (94) and (95),

$$(96) \quad f(\alpha, \beta, \gamma) \leq f(\alpha, \sin \alpha, \gamma).$$

Combining (91) with (92) and (96), we have

$$\begin{aligned}
 (97) \quad f(\alpha, \beta, \gamma) &\leq \max\{f(\alpha, \beta, 0), f(\alpha, \beta, \gamma^+)\} \\
 &\leq \begin{cases} \max\{f(\alpha, \sin \alpha, 0), f(\alpha, \sin \alpha, \gamma^+)\} & \text{if } 0 < \alpha < \pi/2, \\ \max\{f(\alpha, 0, 0), f(\alpha, 0, \gamma^+)\} & \text{if } \pi/2 \leq \alpha < \pi, \end{cases}
 \end{aligned}$$

which yields inequality (44).

7.5. Verify inequalities (46), (47), (48), and (49). Let $z = (\alpha + \sin \alpha)/4$. Since $0 < z < \pi/4$, we have $1 < \frac{z}{\sin z} < 1.111$. Furthermore,

$$\frac{dz}{d\alpha} = \frac{d((\alpha + \sin \alpha)/4)}{d\alpha} = 1/4 + \cos \alpha/4$$

and

$$\frac{d(\frac{z}{\sin z})}{dz} = \frac{1}{\sin z} - \frac{z \cos z}{(\sin z)^2} \leq \frac{1}{\sin z} - \frac{\cos z}{\sin z} = \tan(z/2) < 0.415.$$

Recall that

$$\gamma^+ = \frac{3 \sin \alpha - \alpha}{4} + \arcsin \left(\frac{\alpha + \sin \alpha}{4 \lambda \sin(\frac{\alpha + \sin \alpha}{4})} \right) = \frac{3 \sin \alpha - \alpha}{4} + \arcsin \left(\frac{z}{\lambda \sin z} \right).$$

So

$$\begin{aligned} \left| \frac{d(\gamma^+)}{d\alpha} \right| &\leq \left| \frac{3 \cos \alpha - 1}{4} + \frac{1}{\lambda \sqrt{1 - (\frac{z}{\lambda \sin z})^2}} \frac{d(\frac{z}{\sin z})}{dz} \frac{dz}{d\alpha} \right| \\ &\leq 1 + \left| \frac{0.415}{\lambda \sqrt{1 - (\frac{z}{\lambda \sin z})^2}} (1/4 + \cos \alpha/4) \right| \\ &\leq 1 + \left| \frac{0.415}{\lambda \sqrt{1 - (\frac{1.111}{\lambda})^2}} (1/4 + 1/4) \right| \\ &< 1.15. \end{aligned}$$

Recall that

$$(98) \quad f(\alpha, \beta, \gamma) = -\lambda(\cos \gamma - \cos \alpha(\cos(\beta - \gamma) + \beta \sin(\beta - \gamma))).$$

We have

$$\begin{aligned} \left| \frac{df(\alpha, 0, 0)}{d\alpha} \right| &= \left| \frac{d(-\lambda(1 - \cos \alpha))}{d\alpha} \right| = |-\lambda \sin \alpha| < 2. \\ \left| \frac{df(\alpha, 0, \gamma^+)}{d\alpha} \right| &= \left| \frac{d(-\lambda(\cos \gamma^+ - \cos \alpha \cos(-\gamma^+)))}{d\alpha} \right| \\ &= \left| \frac{d(-\lambda \cos \gamma^+(1 - \cos \alpha))}{d\alpha} \right| \\ &\leq \lambda \left(\left| \frac{d(\gamma^+)}{d\alpha} \sin \gamma^+(1 - \cos \alpha) \right| + |\sin \alpha \cos \gamma^+| \right) \\ &\leq 1.8(1.15 + 1) < 4, \end{aligned}$$

$$\begin{aligned} \left| \frac{df(\alpha, \sin \alpha, 0)}{d\alpha} \right| &= \left| \frac{d(-\lambda(1 - \cos \alpha \cos(\sin \alpha) - \cos \alpha \sin \alpha \sin(\sin \alpha)))}{d\alpha} \right| \\ &\leq \lambda(|\sin \alpha \cos(\sin \alpha)| + |(\cos \alpha)^2 \sin \alpha \cos(\sin \alpha)| \\ &\quad + |(\sin \alpha)^2 \sin(\sin \alpha)|) \\ &\leq 1.8(1 + 1 + 1) < 6, \end{aligned}$$

$$\begin{aligned}
 & \left| \frac{df(\alpha, \sin \alpha, \gamma^+)}{d\alpha} \right| \\
 &= \left| \frac{d(-\lambda(\cos \gamma^+ - \cos \alpha \cos(\sin \alpha - \gamma^+) - \cos \alpha \sin \alpha \sin(\sin \alpha - \gamma^+)))}{d\alpha} \right| \\
 &= \left| \frac{d(-\lambda(\cos \gamma^+ - \cos \alpha \cos(\sin \alpha - \gamma^+) - \frac{\sin(2\alpha)}{2} \sin(\sin \alpha - \gamma^+)))}{d\alpha} \right| \\
 &\leq \lambda \left(\left| \frac{d(\gamma^+)}{d\alpha} \sin \gamma^+ \right| + |\sin \alpha \cos(\sin \alpha - \gamma^+)| \right. \\
 &\quad \left. + \left| \cos \alpha \sin(\sin \alpha - \gamma^+) \left(\cos \alpha - \frac{d(\gamma^+)}{d\alpha} \right) \right| + |\cos(2\alpha) \sin(\sin \alpha - \gamma^+)| \right. \\
 &\quad \left. + \left| \frac{\sin(2\alpha)}{2} \cos(\sin \alpha - \gamma^+) \left(\cos \alpha - \frac{d(\gamma^+)}{d\alpha} \right) \right| \right) \\
 &< 1.8(1.15 + 1 + (1 + 1.15)) + 1 + (1 + 1.15)/2 < 12.
 \end{aligned}$$

Also

$$\begin{aligned}
 \left| \frac{d(\sin \alpha - \alpha \cos \alpha - \frac{2\varphi}{3} - \frac{2\varphi}{3} \cos \alpha)}{d\alpha} \right| &= \left| \alpha \sin \alpha + \frac{2\varphi}{3} \sin \alpha \right| \leq \pi + \frac{2\varphi}{3} < 4, \\
 \left| \frac{d(\sin \alpha - \alpha \cos \alpha - \frac{2\varphi}{3} - \frac{4\varphi}{3} \cos \alpha)}{d\alpha} \right| &= \left| \alpha \sin \alpha + \frac{4\varphi}{3} \sin \alpha \right| \leq \pi + \frac{4\varphi}{3} < 4.
 \end{aligned}$$

Therefore the Lipschitz constants are

$$\begin{aligned}
 \left| \frac{dg_1(\alpha)}{d\alpha} \right| &= \left| \frac{d(\sin \alpha - \alpha \cos \alpha - \frac{2\varphi}{3} - \frac{2\varphi}{3} \cos \alpha)}{d\alpha} \right| + \left| \frac{df(\alpha, 0, 0)}{d\alpha} \right| < 4 + 2 < 16, \\
 \left| \frac{dg_2(\alpha)}{d\alpha} \right| &= \left| \frac{d(\sin \alpha - \alpha \cos \alpha - \frac{2\varphi}{3} - \frac{2\varphi}{3} \cos \alpha)}{d\alpha} \right| + \left| \frac{df(\alpha, 0, \gamma^+)}{d\alpha} \right| < 4 + 4 < 16, \\
 \left| \frac{dg_3(\alpha)}{d\alpha} \right| &= \left| \frac{d(\sin \alpha - \alpha \cos \alpha - \frac{2\varphi}{3} - \frac{2\varphi}{3} \cos \alpha)}{d\alpha} \right| + \left| \frac{df(\alpha, \sin \alpha, 0)}{d\alpha} \right| < 4 + 6 < 16, \\
 \left| \frac{dg_4(\alpha)}{d\alpha} \right| &= \left| \frac{d(\sin \alpha - \alpha \cos \alpha - \frac{2\varphi}{3} - \frac{2\varphi}{3} \cos \alpha)}{d\alpha} \right| + \left| \frac{df(\alpha, \sin \alpha, \gamma^+)}{d\alpha} \right| < 4 + 12 = 16.
 \end{aligned}$$

Now we can use a simplified version of the Piyavskii algorithm [16] for Lipschitz optimization to verify that $g_i(\alpha) < 0, 1 \leq i \leq 4$. Algorithm **Bound**(g_i, s, t) will either find a value $g_i(\alpha) \geq 0$ in the given range or return an upper bound on the value of g_i in range $[s, t]$ that is less than 0. For $1 \leq i \leq 4$, we run **Bound**(g_i, s, t) with s and t set to be the appropriate lower and upper bound on the range of α , where $g_i(0)$ is set to be $\lim_{\alpha \rightarrow 0} g_i(\alpha)$. We verify that indeed $g_i(\alpha) < 0, 1 \leq i \leq 4$. This completes the verification of inequalities (46), (47), (48), and (49).

Acknowledgments. The author thanks the anonymous reviewers for their valuable comments, which improved the quality of the paper. The author is also grateful to Iyad Kanj and Shiliang Cui for helpful discussions related to the paper.

ALGORITHM **Bound**(g_i, s, t) for $1 \leq i \leq 4$.

1. **if** $g_i(s) \geq 0$ or $g_i(t) \geq 0$ **return** $\max\{g_i(s), g_i(t)\}$.
2. $\text{apex} = \max\{g_i(s), g_i(t)\} + 16 * (t - s)/2$
3. **if** $\text{apex} \geq 0$, **do**:
 - 3.1. $\text{apex} = \max\{\mathbf{Bound}(g_i, s, (s + t)/2), \mathbf{Bound}(g_i, (s + t)/2, t)\}$
4. **return** apex

REFERENCES

- [1] R. BENSON, *Euclidean Geometry and Convexity*, McGraw-Hill, New York, 1966.
- [2] P. BOSE, L. DEVROYE, M. LÖFFLER, J. SNOEYINK, AND V. VERMA, *Almost all Delaunay triangulations have stretch factor greater than $\pi/2$* , *Comput. Geom.*, 44 (2011), pp. 121–127.
- [3] P. BOSE, J. GUDMUNDSSON, AND M. SMID, *Constructing plane spanners of bounded degree and low weight*, *Algorithmica*, 42 (2005), pp. 249–264.
- [4] P. BOSE AND M. SMID, *On Plane Geometric Spanners: A Survey and Open Problems*, manuscript, 2010; available online from people.scs.carleton.ca/~michiel/surveyplanespanners.pdf.
- [5] P. CHEW, *There are planar graphs almost as good as the complete graph*, *J. Comput. System Sci.*, 39 (1989), pp. 205–219.
- [6] S. CUI, I. A. KANJ, AND G. XIA, *On the stretch factor of Delaunay triangulations of points in convex position*, *Comput. Geom.*, 44 (2011), pp. 104–109.
- [7] D. DOBKIN, S. FRIEDMAN, AND K. SUPOWIT, *Delaunay graphs are almost as good as complete graphs*, in *Proceedings of the 28th Annual Symposium on Foundations of Computer Science (FOCS)*, 1987, pp. 20–26.
- [8] D. DOBKIN, S. FRIEDMAN, AND K. SUPOWIT, *Delaunay graphs are almost as good as complete graphs*, *Discrete Comput. Geom.*, 5 (1990), pp. 399–407.
- [9] J. GUDMUNDSSON, C. LEVCOPOULOS, AND G. NARASIMHAN, *Fast greedy algorithms for constructing sparse geometric spanners*, *SIAM J. Comput.*, 31 (2002), pp. 1479–1500.
- [10] I. A. KANJ, L. PERKOVIĆ, AND G. XIA, *On spanners and lightweight spanners of geometric graphs*, *SIAM J. Comput.*, 39 (2010), pp. 2132–2161.
- [11] W. KAPLAN, *Maxima and Minima with Applications: Practical Optimization and Duality*, John Wiley, New York, 1999.
- [12] J. KEIL AND C. GUTWIN, *The Delaunay triangulation closely approximates the complete Euclidean graph*, in *Proceedings of the 1st Workshop on Algorithms and Data Structures (WADS)*, 1989, pp. 47–56.
- [13] J. KEIL AND C. GUTWIN, *Classes of graphs which approximate the complete Euclidean graph*, *Discrete Comput. Geom.*, 7 (1992), pp. 13–28.
- [14] X.-Y. LI, G. CALINESCU, P.-J. WAN, AND Y. WANG, *Localized Delaunay triangulation with application in ad hoc wireless networks*, *IEEE Trans. Parallel Distrib. Systems*, 14 (2003), pp. 1035–1047.
- [15] G. NARASIMHAN AND M. SMID, *Geometric Spanner Networks*, Cambridge University Press, Cambridge, UK, 2007.
- [16] R. J. VANDERBEI, *Extension of Piyavskii’s algorithm to continuous global optimization*, *J. Global Optim.*, 14 (1997), pp. 205–216.
- [17] G. XIA AND L. ZHANG, *Toward the tight bound of the stretch factor of Delaunay triangulations*, in *Proceedings of the 23rd Canadian Conference on Computational Geometry (CCCG)*, 2011.